



## Review

## On silsesquioxanes' accuracy as molecular models for silica-grafted complexes in heterogeneous catalysis

Elsje Alessandra Quadrelli\*, Jean-Marie Basset

Université de Lyon, Équipe de Chimie Organométallique de Surface, ICL, UMR C2P2 CNRS-Université Lyon 1-CPE Lyon, 43 Boulevard du 11 Novembre 1918, 69616 Villeurbanne, France

## Contents

1. Introduction, goal and scope.....	708
2. Analogy between oxidic supports and silsesquioxane molecules.....	709
2.1. Silsesquioxane as models of silica surfaces.....	709
2.2. Element-containing silicates and zeolites modelled by modified silsesquioxanes.....	710
3. Structural and activity analogy between silica-grafted catalysts and silsesquioxane derivatives.....	711
3.1. Group 3 and lanthanides.....	711
3.1.1. Lanthanide amides as Diels–Alder cyclization catalysts.....	711
3.2. Group 4.....	711
3.2.1. Titanium-based epoxidation catalysts.....	711
3.2.2. Titanocene-, zirconocene- and related half-sandwich based polymerization catalysts.....	713
3.2.3. Ziegler–Natta type polymerization catalysts.....	715
3.2.4. Group 4 alkyls and hydrides (M = Zr, Ti, Hf) for catalytic hydrocarbon transformations.....	715
3.2.5. Zirconium acetylacetonate as an acrylate trans-esterification catalyst.....	718
3.3. Group 5.....	718
3.3.1. Vanadium oxides for selective oxidations.....	718
3.3.2. Alkylated vanadium oxides for olefin polymerization.....	718
3.4. Group 6.....	719
3.4.1. Chromium-based models for polymerization catalysts.....	719
3.4.2. Molybdenum-oxo dehydrogenation catalysts.....	720
3.4.3. Molybdenum and tungsten imido carbene as olefin metathesis catalysts.....	720
3.4.4. Molybdenum alkylidyne for alkyne metathesis and homodimerization catalyst.....	721
3.5. Group 7.....	723
3.5.1. Olefin metathesis Re-carbene catalysts.....	723
3.6. Group 8.....	723
3.6.1. Fe-based oxidation catalysts.....	723
3.7. Group 9.....	723
3.7.1. Rhodium-based catalysts for hydroformylation.....	723
3.8. Group 10.....	723
3.8.1. Platinum catalysts for hydrogenation.....	723
3.9. Group 11.....	724
3.9.1. Gold on silica catalysts.....	724
3.10. Group 12.....	724
3.10.1. Zinc catalysts.....	724
3.11. Group 13.....	725
3.11.1. Models of silica-grafted organoboranes for floating Zr polymerization catalysts.....	725
3.11.2. Al-based catalysts for polymerization.....	725
3.11.3. Ga-modified silsesquioxanes as models for doped zeolites.....	725
3.12. Group 14.....	725
3.12.1. Tin catalysts for oxidation.....	725
4. Conclusions.....	726
References.....	727

\* Corresponding author. Tel.: +33 4 72431808; fax: +33 4 72431795.

E-mail addresses: [quadrelli@cpe.fr](mailto:quadrelli@cpe.fr) (E.A. Quadrelli), [basset@cpe.fr](mailto:basset@cpe.fr) (J.-M. Basset).

## ARTICLE INFO

## Article history:

Received 11 June 2009

Accepted 27 September 2009

Available online 2 October 2009

Both authors want to dedicate this article to Fausto Calderazzo, their common mentor, their common father in chemistry.

## Keywords:

Silsesquioxane

Silica

Surface organometallic chemistry

Heterogeneous catalysts

Molecular models

## ABSTRACT

The achievement of a structure–activity relationship for heterogeneous catalysts is a desirable step for improving existing catalysts or for predicting new catalytic reactions. This article reviews the use of silsesquioxanes (POSS) organometallic complexes as molecular models for silica-grafted catalytic centers. It will show that POSS complexes, within some limits, have substantially contributed to gaining better molecular-level understanding of surface reactions and catalysts activity.

© 2009 Elsevier B.V. All rights reserved.

## 1. Introduction, goal and scope

Catalysis is the number one technology in chemical industry and petroleum refining. In the future, one may reasonably expect that catalysis will be among the leading solution for meeting the new, global, and intimately related challenges of environment and energy. The advantages of catalytic processes are due to the relatively mild reaction conditions, their cost efficiency, and their environmentally friendly character. Heterogeneous catalysis is the most commonly used of the three possible catalytic systems (the other ones being homogeneous and enzymatic), has the longest history in manmade chemicals, and remains the most widespread solution in industrial processes, in part due to ease of catalyst separation from reaction medium. Nevertheless, heterogeneous catalysis still suffers from some drawbacks. Sometimes it is not selective enough, sometimes it produces undesired products (like CO<sub>2</sub>, NO<sub>x</sub> or particles), sometimes it requires high temperatures which are energy demanding, sometimes the catalyst lifetime is too short which is not economical, and sometimes its regeneration procedures are complicated, etc. Some of the reasons for these drawbacks are inherent to the “heterogeneous” character of these materials. The multiplicity of active sites in terms of structure and their low concentration prevent the achievement of a structure–activity relationship, a desirable step for improving existing catalysts or for predicting new catalytic reactions. Nowadays, spectacular progress in the synthesis of new and well-defined materials is being observed. It is now possible to perform rational design and synthesis, thanks to supramolecular and sol–gel chemistry, of well-defined supports with the expected structure, acidity, porosity or shape in the field of oxides. Despite these improvements, the synthesis of materials which are more and more precisely defined from the atomic level, to the nanolevel and to the centimetre level, has not yet achieved optimum catalytic activity, selectivity, lifetime, and so on.

The “surface organometallic chemistry” (SOMC) [1,2] field has been developed to propose a well-defined approach to the conception and synthesis of heterogeneous catalysts, either on traditional or on novel supports. The SOMC field concerns the grafting of any organometallic or coordination compound onto any surface. By surfaces we mean those of simple oxides (from non-porous, to mesoporous, up to zeolitic materials), those of metals (from unsupported nanoparticles to supported ones, up to single crystals of metals), those of carbon (from carbon black to graphene, to carbon nanotubes), those of carbides, nitrides, etc.; and the grafting of organometallic compounds aims at the synthesis of “single site” organometallic heterogeneous catalysts. The detailed knowledge of

the structure of the active site which results from a careful structural determination, leads to the elucidation of elementary steps of heterogeneous catalysis. A structure–activity relationship can thus be achieved in several cases: for example in the case of the most commonly used supports, that is those of oxides, we have contributed to reporting a new generation of catalysts, catalytic reactions, and have improved existing catalysts related to energy and environment. Nevertheless, such a field still suffers from a lack of tools to characterize the so-called single sites, even if a variety of techniques coming from surface science and molecular chemistry have emerged: *in situ* IR, *in situ* <sup>1</sup>H, <sup>13</sup>C NMR, 2D NMR, EXAFS, surface microanalysis, and determination of the stoichiometry of surface reactions.

The focus of the review will be on the use of molecular models to mimic and better understand the surfaces of inorganic oxide supports and their related surface-grafted organometallic fragments. Such molecular models can help – and have helped as this review will show in the case of silica – gain insight in the molecular understanding of the whole catalytic act occurring on heterogeneous catalysts. One should not forget that heterogeneous catalysis is a molecular phenomenon occurring on a surface and surface organometallic fragments are real reaction intermediates in most cases. For silica, molecular models of surface-grafted organometallic derivatives have been obtained with model ligands such as mono- or polysiloxy [3,4], calixarenes [5–7], heteropolyanions [8], and trisamidates [9]. Among these ligands, the siloxy molecules belonging to the silsesquioxane family – or more accurately to the polyhedral oligomeric silsesquioxane (POSS) family, characterized by a self-organized cage-like structure and reactive silanol moieties – have asserted themselves among the most convincing analogues of silica’s surface silanols. The goal of the review will be to present the structural proof and reactivity analogy that support such comparison. Where possible, the direct comparison between analogous experimental properties will be carried out (solid vs. solution NMR; EXAFS vs. single crystal X-ray diffraction, heterogeneous vs. homogeneous catalytic TOF and TON, etc.). The use of POSS in computational studies for theoretical molecular modelling the SiO<sub>2</sub> clusters [10] and possibly silica-based catalysts [11,12], will not be tackled here. The scope of the review will also be restricted to POSS-based systems which (i) can be considered a close molecular analogue of active heterogeneous catalyst, (ii) have well-defined structural data both for the molecular and for silica-supported species, and (iii) have direct M–OSi bond, in other words, the heterogeneous catalysts included here do not take into account the heterogenized homogeneous ones, obtained for example by the tethering approach (that is the use of organic bifunctional

tethers whose ‘tail’ grafts to the support while its ‘head’ coordinates the active catalytic metals), albeit silsesquioxane have been successfully applied also in these cases [13–15]. In the context of silsesquioxane-based catalysts, this work is in continuation of reviews showing metallorganic derivatives of POSS as catalysts in their own right [4,16], or used as models for heterogeneous olefin polymerization catalysts [17,18] and olefin metathesis catalysts [19], or as models for surface organometallic chemistry [1,2,20]. For silsesquioxane applications beside catalysis and modelling thereof, the reader is referred to reviews focusing on silsesquioxane synthesis [21,22], their use as ligands in inorganic and organometallic chemistry [3,23–25], or their application as material-science precursors [26–28], that will provide a broader view of all the much larger bulk of work revolving around silsesquioxanes.

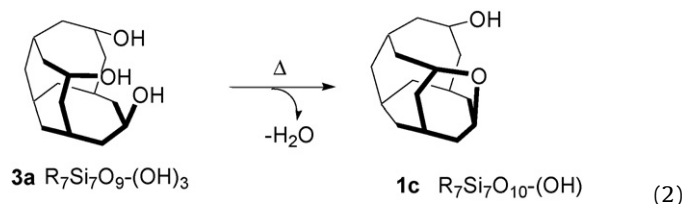
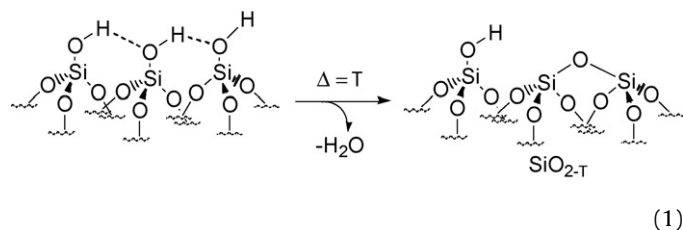
## 2. Analogy between oxidic supports and silsesquioxane molecules

### 2.1. Silsesquioxane as models of silica surfaces

“Notwithstanding the very simple chemical formula of silicon dioxide, silica exists in a very large number of different forms” [29]. To attempt a description of the structural features that can be modelled with silsesquioxane, we will limit ourselves to surface silanols and their classification in isolated, vicinal or geminal (Chart 1) [29–31], since they are the reactive sites upon which grafting of the organometallic precursor usually occurs in the synthesis of silica-supported heterogeneous catalysts and whose nature and concentration influence the nature of the grafted organometallic moiety [1]. In the polyhedral oligomeric silsesquioxanes of interest here (Chart 1), the cubic framework of the molecular cage is made of Si–R moieties in the corner positions and oxygen atoms between them (R being typically cyclopentyl,  $c\text{-C}_5\text{H}_9$  or cyclohexyl,  $c\text{-C}_6\text{H}_{11}$ , rings). The trisilanol  $(\text{C}_6\text{H}_{11})_7\text{Si}_7\text{O}_9(\text{OH})_3$ , **3a**– $\text{C}_6\text{H}_{11}$ , the first for which a convenient high-yield (and 6-month long!) synthesis was reported [32], is obtained by controlled hydrolytic condensation of trichlorocyclohexylsilane. Since then, many other POSS-based derivatives have been reported, with substitution in the number of atoms forming the cages, tethers, number of silanols, etc. The silsesquioxanes of interest here have been chosen for their analogy with silica’s silanols, with molecular type and number of reactive silanols that can vary from one (**1a**–**1c**), to two (**2a**–**2c**) three (**3a**) or four (**4a**). In fact, by judicious control of the hydrolytic condensation reaction conditions, it is possible to avoid the fully condensed polyhedra  $\text{R}_8\text{Si}_8\text{O}_{12}$  or  $\text{R}_6\text{Si}_6\text{O}_9$ , and steer the reaction to prevalently open cages with “dangling” Si–OH silica-like moieties. Subsequent silylation [33], base-catalyzed cleavage or cyclocondensations allow the further tuning of the number and nature of the available silanols on the partially condensed silsesquioxanes. For example the disilanols  $\text{R}_8\text{Si}_8\text{O}_{10}(\text{OH})_2$ , **2a**,  $\text{R}_7\text{Si}_7\text{O}_9(\text{OSiMe}_3)(\text{OH})_2$ , **2b**, are reported as model of vicinal surface silanols, while disilanol  $\text{R}_7\text{Si}_7\text{O}_9(\text{OSiMe}_3)(\text{OH})_2$ , **2c**, has been synthesized to model geminal silanols [34]. Monosilanols  $\text{R}_7\text{Si}_7\text{O}_9(\text{OSiMe}_3)_2(\text{OH})$ , **1b**,  $\text{R}_7\text{Si}_7\text{O}_{10}(\text{OH})$ , **1c**, can be obtained to model the isolated surface silanol. Formally connected to the same family of POSS, the monosilanol based on the closed structure  $\text{R}_7\text{Si}_8\text{O}_{12}(\text{OH})$ , **1a**, is also a model for isolated surface silanols [35]. Overall, these models along with the tris- and tetrasilanols, models of fully hydroxylated surfaces, yield the starting molecules used as models of various type for reactive silanols molecular model for isolated, vicinal, and geminal present on silica surface (Chart 1).

The close analogy between vicinal silica surface silanols and incompletely condensed silsesquioxanes was first highlighted by Feher’s seminal work [32]. The major contribution of the work

was twofold: (i) it proposed a novel, easy, and high-yield synthesis for the known compound  $(c\text{-C}_6\text{H}_{11})_7\text{Si}_7\text{O}_9(\text{OH})_3$ , **3a**– $\text{C}_6\text{H}_{11}$  (see above), and most importantly for the research field of interest in this review (ii) it offered a clear description of the analogy between the silsesquioxane **3a**– $\text{C}_6\text{H}_{11}$  and the surface of a fully hydrated silica slab. The reported analysis of the X-ray data proved that the molecular structure of trisilanol  $(c\text{-C}_6\text{H}_{11})_7\text{Si}_7\text{O}_9(\text{OH})_3$ , **3a**– $\text{C}_6\text{H}_{11}$ , compared strikingly well to a portion of a (1 1 1)β-cristobalite face: both siliceous cavities are formed by 12-member siloxane rings, with silicon atoms arranged in a chair conformation overlapping over either three or four layers, respectively, resulting in a similar cavity depth (3.8 Å vs. 5.1 Å) and Si–Si distances (4.9 Å vs. 5.04 Å). The OH⋯OH distance in the silsesquioxane **3a**– $\text{C}_6\text{H}_{11}$  is 4.0 Å and the projected silanol density is 4.8 OH/nm<sup>2</sup> [32], which correlates well with the high-end experimental data of 4.5–5 OH/nm<sup>2</sup> measured for fully hydroxylated silica surfaces [36]. Lower densities are measured for silica that have undergone thermal treatment under vacuum, because of the loss of water between adjacent surface silanols (reaction (1), the temperature *T* being called the dehydroxylation temperature, and the ensuing silica noted as  $\text{SiO}_{2-T}$ ). Similarly, silsesquioxane can model such chemistry since trisilanol **3a**– $\text{C}_6\text{H}_{11}$  undergoes dehydration to the cyclocondensed monosilanol complex **1c** upon heating (reaction (2)) [32]:



The analogy between silica surface silanols and silsesquioxanes is also spectroscopic. Infrared spectra of silica after extensive thermal treatment, and hence extensive dehydroxylation (reaction (1)), show a sharp peak at 3750 cm<sup>−1</sup>, assigned to truly isolated (non-acidic) [≡SiOH] silanols; likewise, monosilanol silsesquioxane of type **1** gives both in solution and in solid-state IR spectra a sharp band around 3700 cm<sup>−1</sup> [35], while strongly hydrogen-bonded trisilanol of type **3** displays  $\nu(\text{OH}) = 3158$  (nujol), and 3217 (CCl<sub>4</sub>) cm<sup>−1</sup> [34].

The long-range effect of adjacent siloxide functionalities on the stretching vibration of isolated silanols on silica was indicated by the development of a series of POSS monosilanols of type **1b**, where the two capping SiMe<sub>3</sub> groups have been replaced by a variable-size methyl substituted siloxane ring: FTIR data showed that hydrogen bonding preferentially occurred between the silanol and the flexible 12 member siloxane ring, suggesting that such effect is present also on silica, with interesting implication for subsequent catalytic activities (*vide infra*) [37].

Silsesquioxane **2c** was used to mimic and help the solid-state assignment of surface geminal silanols IR stretching frequencies  $\nu(\text{OH})$  [34]; the study also highlighted the different chemical nature of the two *endo* and *exo* Si–OH moieties in the silsesquioxane **2c** [34], possibly explaining the observed chemical behavior of geminal silanol on silica surface, that rather counter-intuitively behaves more like an isolated surface silanol than like a disilanol. Spectro-

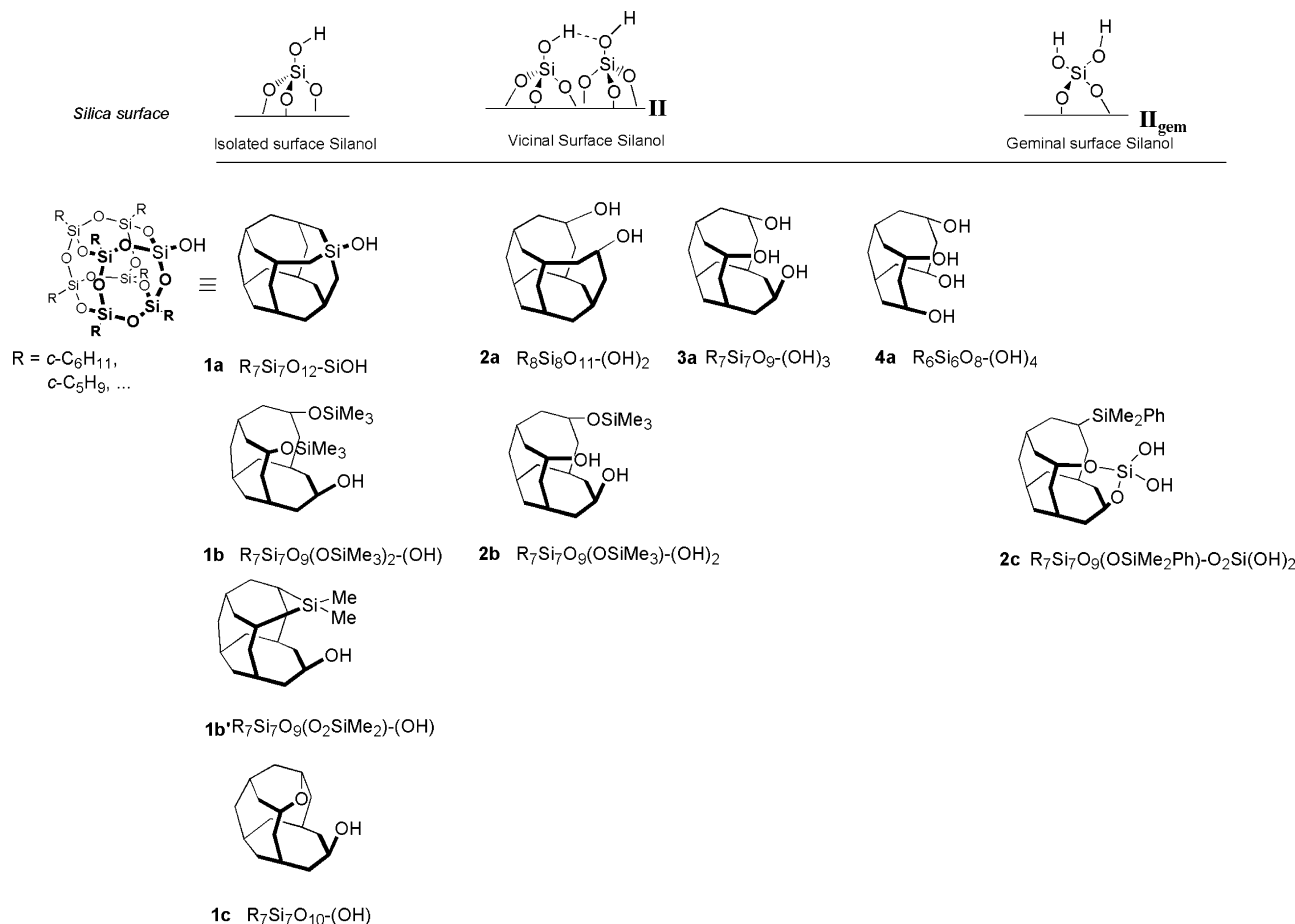


**Chart 1.** Overview of the main silsesquioxanes used as molecular models to isolated, vicinal, and geminal surface silanols found on silica.

scopic  $^1H$  and  $^{29}Si$  NMR measurements also compare well between silsesquioxanes [34] and silica surface silanols [22].

Silsesquioxanes acidity compares less well with that of the silicas. While NaOH deprotonates truly isolated silica silanols (thus  $pK_a = ca. 7$ ) [29], solution indicators measure weaker ion-pair acidity for silsesquioxanes (8.9 for **1a** and 9.6 for **1b'**) [34]. Nevertheless, these values remain closer to silica than the acidities of simpler molecular models such as  $Ph_3SiOH$  ( $pK_a = 10.8$ ), indicating that the silsesquioxane cage does provide some of the electronegative  $CF_3$ -like electron withdrawing effect of silica bulk on surface silanol. The silica–silsesquioxane analogy becomes stronger if one looks at hydrogen-bonded systems: the increase in acidity observed for poly-hydrogen-bonded surface silanols [29] is also observed for silsesquioxanes bearing multiple hydrogen-bonded silanols such as **3a** and **4a** ( $pK_{ib} = ca. 7.6$ ) [34], and is absent in vicinal disilanols ( $pK_{ib}(\mathbf{2b}) = ca. 9.5$ ) or, even more so, in geminal disilanols ( $pK_{ib}(\mathbf{2c}) = ca. 10.2$ ). This difference in acidity also affects changes in reactivity. Partially silylated silsesquioxanes (such as mono and bis trimethylsilyl (TMS) substituted compounds **2b** and **1b'**) display enhanced silylation reactivity with respect to the parent TMS-free trisilanol compound **3a**, thus leading one to suggest that the most reactive sites for silylation of hydroxylated silica surfaces might be the silanols moieties involved in at least three-membered mutually bonded hydrogen-nested hydroxyls [33]. The difference in acidity discussed above is part of the explanation. Similarly, the investigation of the reaction of  $SbMe_5$  with parent trisilanol **3a** and variously silylated silsesquioxanes, among which are **1b**, **1c**, and **2b**, suggested that nested hydrogen-bonded surface sites are more prone to reaction with organometallic nucleophiles than isolated silanols [38].

## 2.2. Element-containing silicates and zeolites modelled by modified silsesquioxanes

Molecular models for Al/Si/O frameworks were obtained from reaction of trimethylaluminum with trisilanol silsesquioxane **3a** to give alkyl-free Al-capped silsesquioxane dimer [39], a model for Lewis acidic aluminum sites in zeolites. The dimer can be transformed in an anionic aluminosilsesquioxane salt, formally connected to type A zeolite topology (Chart 2) [40]. Reactions of  $AlMe_3$  or  $AlCl_3$  with bisilanol of type **2** lead to the Brønsted acidic aluminosilsesquioxane  $[(c-C_5H_9)_7Si_7O_{11}(OSiMe_3)]Al[(c-C_5H_9)_7Si_7O_1(OSiMe_3)(OH)]$ , model for acidic sites in zeolites and aluminosilicates [41], and to anionic aluminosilicate, model of the tetrahedral aluminum sites in aluminosilicates [42]. The Al–O distances in the latter molecular complex, ranging from 1.725(7) to 1.788(6) Å, compare well with the EXAFS-determined 1.75 Å Al–O distances found in Na-FAU, where the environment around each aluminum atom is almost perfectly tetrahedral [43]. The stretching vibration of the former,  $\nu(OH) = 3150\text{ cm}^{-1}$  in  $C_4Cl_6$ , suggests stronger hydrogen bonding than in the zeolite solids, where  $\nu(OH) = 3550\text{ cm}^{-1}$  for hydrogen-bonded hydroxyl moieties of HY zeolite, shifted by about  $100\text{ cm}^{-1}$  with respect to their non-bridged analogues [ $\nu(OH) = 3650\text{ cm}^{-1}$ ] [41]. The IR spectra of silsesquioxane were further applied to model zeolite defective nests [44], with the limitation caused by the hydrogen-bonded silsesquioxane dimers in the solid state and in solution [34].

Other group 13 element-containing zeolites and silicates have been successfully modelled with silsesquioxanes [45], and given their important role in catalysis will be discussed in the next section, which is focused on highlighting the accuracy of metal-

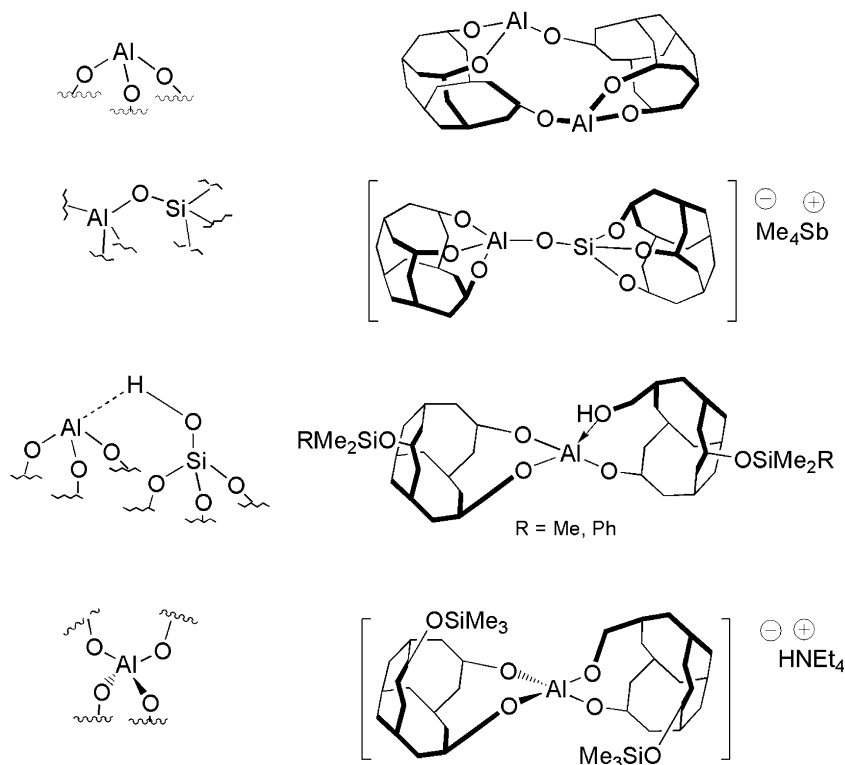


**Chart 2.** Comparison between aluminum sites in alumina and silica alumina supports (left) and possible silsesquioxane-based model (right).

containing coordination and organometallic derivatives of POSS, also known as polyhedral *metal* silsesquioxanes (POMS), as molecular models for silica-supported catalytic systems.

### 3. Structural and activity analogy between silica-grafted catalysts and silsesquioxane derivatives

#### 3.1. Group 3 and lanthanides

##### 3.1.1. Lanthanide amides as Diels–Alder cyclization catalysts

Silica-supported group 3 and rare-earth amides  $[(\equiv\text{SiO})\text{Ln}\{\text{N}(\text{SiMe}_3)_2\}]$  ( $\text{Ln} = \text{Y}, \text{La}, \text{Nd}$  and  $\text{Sm}$ ) are phenylacetylene dimerization catalysts [46]. The monosiloxy derivatives are obtained by grafting the peramido precursor  $\text{Ln}\{\text{N}(\text{SiMe}_3)_2\}_3$  with highly dehydroxylated silica,  $\text{SiO}_2-700$ , while lower dehydroxylation temperature yield a mixture of surface products [47]. The mixture of bisiloxy and monosiloxy derivatives  $[(\equiv\text{SiO})_2\text{Ln}\{\text{N}(\text{SiHMe}_2)_2\}]$  and  $[(\equiv\text{SiO})\text{Ln}\{\text{N}(\text{SiHMe}_2)_2\}]$  is obtained from the reaction of  $\text{Ln}\{\text{N}(\text{SiHMe}_2)_2\}_3$  ( $\text{Ln} = \text{Y}$  and  $\text{Nd}$ ) with mesoporous silica (MCM-41) dehydroxylated at 350 °C [48].

Straight-forward reaction between the tris(trimethylsilylamido) derivatives of  $\text{Ln} = \text{Y}, \text{La}, \text{Pr}, \text{Eu}$ , and  $\text{Yb}$  with the trisilanol silsesquioxane **3a** failed to give molecules comparable to the silica-grafted amides above, since only amide-free trisilanol and/or bis-THF adduct  $[(\text{C}_6\text{H}_{11})_7\text{Si}_7\text{O}_{12}]\text{Ln}(\text{THF})_2$  could be recovered [49]. A better silsesquioxane model for silica-supported silylamide yttrium derivative has been obtained from a lithium salt of  $\text{C}_6\text{H}_{11}$ -**3a** (Scheme 1), but the modelling is very approximate since the silsesquioxane product  $[(\text{C}_6\text{H}_{11})_7\text{Si}_7\text{O}_{12}\text{Li}_4]\text{Yb}\{\text{N}(\text{SiMe}_3)_2\}$  is a lithium salt [50].

Silica-grafted lanthanide silylamides were used as precursors to surface  $\beta$ -diketonate complexes  $[(\equiv\text{SiO})_n\text{Ln}(\text{tBu-COCHCO-}^n\text{C}_3\text{F}_7)_m(\text{THF})_l]$  ( $\text{Ln} = \text{Sc}, \text{Y}$  and  $\text{La}$ ), successful heterogeneous catalysts for the Danishefsky cyclization of *t*-1-methoxy-3-

trimethylsilyloxy-1,3-butadiene with benzaldehyde [51]. The closest silsesquioxane model is  $[(\text{C}_6\text{H}_{11})_7\text{Si}_7\text{O}_{11}\text{Si}(\mu\text{-O})\text{Sc}(\text{acac})_2]_2$ , obtained by reaction of  $\text{Cp}^*\text{Sc}(\text{acac})_2$  ( $\text{acac} = \text{MeCOCHCOMe}$ ) with monosilanol **1a**- $\text{C}_6\text{H}_{11}$  but no catalysis is reported [52].

#### 3.2. Group 4

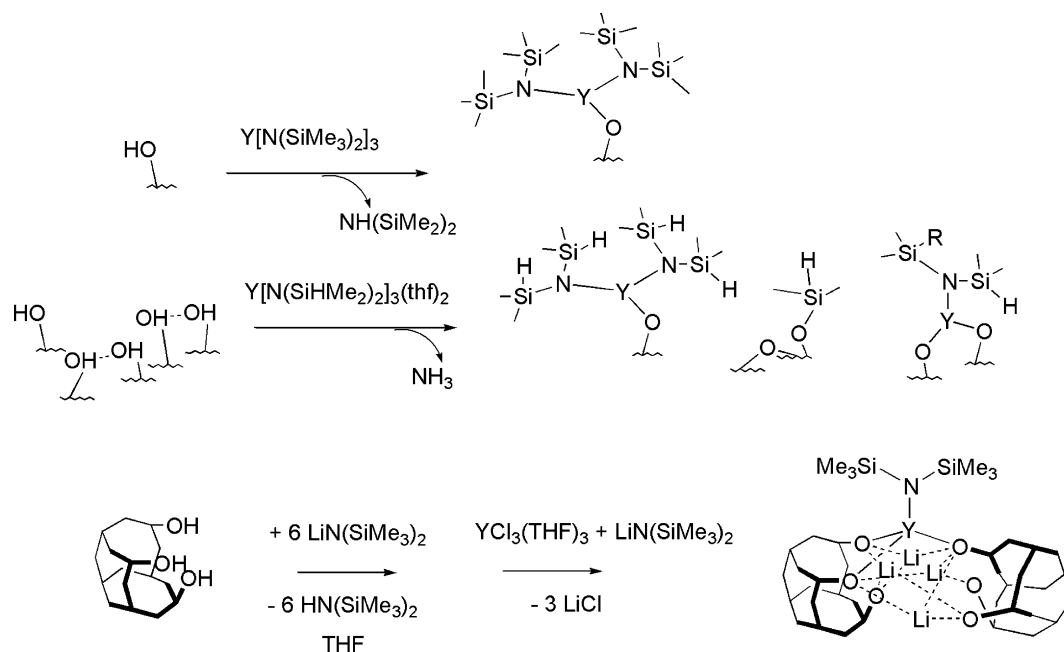
##### 3.2.1. Titanium-based epoxidation catalysts

The trisiloxy complex  $[(\equiv\text{SiO})_3\text{TiOH}]$  is believed to be one of the dominant active surface species in silica-supported titanium(IV) alkoxides and in titanium silicalite-1 industrial epoxidation catalysts [53–58]. Its coordination sphere is reported to expand from four to six during the catalytic cycle to a time-averaged Ti(IV) surface complex  $[(\equiv\text{SiO})_3\text{Ti}(\text{OH}_2)(\text{OOH})]$  active species [56,57].

Silsesquioxane-based molecular models for the tripodally (open lattice) site  $[(\equiv\text{SiO})_3\text{TiOH}]$  were obtained by reaction of various titanium(IV) homoleptic tetraalkoxides  $\text{Ti}(\text{OR})_4$  ( $\text{OR} = \text{OMe}$  and  $\text{OPr}^i$ ) and other Ti(IV)  $\text{TiX}_4$  precursors ( $\text{X} = \text{OSiMe}_3$ ,  $\text{OSiPh}_3$ ,  $\text{OGepH}_3$ ,  $\text{NMe}_2$ , and  $\text{CH}_2\text{Ph}$ ) [59–61] with trisilanol **3a**, or by exchanging the capping X in the Ti(IV) silsesquioxane  $[(\text{R}_7\text{Si}_7\text{O}_9)\text{-O}_3\text{TiX}]$ , ( $\text{R} = \text{C}_5\text{H}_9$  or  $\text{C}_6\text{H}_{11}$ ;  $\text{X} = \text{Cl}$ ,  $\text{OPr}^i$ ) with  $\text{OSnPh}_3$  [57],  $\text{OC}_6\text{H}_5$ ,  $\text{OC}_6\text{H}_4\text{-p-F}$ , or  $\text{OC}_6\text{H}_4\text{-p-NO}_2$  [61]. In the solid state, both a hexacoordinated dimeric methanol adduct and a tetrahedral monomeric species,  $[(\text{C}_5\text{H}_9)_7\text{Si}_7\text{O}_9\text{-O}_3\text{Ti}(\mu\text{-OMe})(\text{MeOH})]_2$ , and  $[(\text{C}_6\text{H}_{11})_7\text{Si}_7\text{O}_9\text{-O}_3\text{TiOSiMe}_3]$ , respectively, have been structurally characterized by X-ray diffraction on single crystal [59,60] yielding measured Ti–O distances in good agreement with the EXAFS-determined (average) Ti–O distances for the analogous heterogeneous silica-bound species both for the tetrahedral and for the octahedral geometry (Table 1).

Some of the above mentioned Ti–silsesquioxanes and some others complexes (Chart 3 for selected examples), which are models for tetrapodal, tripodal, bipodal, or monopodal possible grafted sur-





**Scheme 1.** Analogy between reactions of yttrium silylamide with variously dehydroxylated silicas and trisilanol silsesquioxane.

face species (that is displaying Ti atom with 4, 3, 2, or only 1 bond to the silica), have been tested in cyclohexene or octene epoxidation with tertbutylhydroperoxide. The goal was twofold: (i) try to establish some structure–activity relationships for the molecular species, and (ii) gain insight in the same epoxidation reactions catalyzed by their “role-model” heterogeneous titanium silicalite and Ti-containing mesostructured MCM-41 silica analogues.

The silsesquioxane analogue for the tetrapodal (closed lattice) site heterogeneous species  $[(\equiv\text{SiO})_4\text{Ti}]$ ,  $[(\text{R}_7\text{Si}_7\text{O}_9)(\text{OSiMe}_3)\text{-O}_2\text{TiO}_2\text{-(R}_7\text{Si}_7\text{O}_9)(\text{OSiMe}_3)]$ , obtained by reaction of two equivalents of bisilanol **2b**- $\text{C}_6\text{H}_{11}$  with  $\text{Ti}(\text{CH}_2\text{Ph})_4$ , is a poor catalyst for alkene epoxidation, in line with the expected inefficiency of a closed lattice Ti(IV) center in the heterogeneous catalysts [59].

Replacement of methoxide with bulkier alkoxides in the series  $[(\text{R}_7\text{Si}_7\text{O}_9)\text{-O}_3\text{Ti(OR)}]$  and the ensuing drop in catalytic

activity ( $\text{R}' = \text{Me} > \text{Bu}^n > \text{Pr}^i$ ), suggested that the catalytic activity of the silsesquioxane models is positively correlated with the steric accessibility of the tetracoordinated Ti(IV) center [60]. The influence of steric congestion on the catalytic performance of Ti(IV)-based silsesquioxanes was also shown by the series of bisilanol derivatives of **2b**,  $[(\text{C}_5\text{H}_9)_7\text{Si}_7\text{O}_9(\text{OSiMe}_3)\text{-O}_2\text{Ti(OR')}_2]$  and  $[(\text{C}_5\text{H}_9)_7\text{Si}_7\text{O}_9(\text{OSiMe}_3)\text{-O}_2\text{Ti(BINOL)}]$ , of the monosilanol derivatives of **1b**,  $[(\text{C}_5\text{H}_9)_7\text{Si}_7\text{O}_9(\text{OSiMe}_3)_2\text{-OTi(OR')}_3]$  and  $[(\text{C}_5\text{H}_9)_7\text{Si}_7\text{O}_9(\text{OSiMe}_3)_2\text{-OTi(OR')(BINOL)}]$ , and of **1c**  $[(\text{C}_5\text{H}_9)_7\text{Si}_7\text{O}_{10}\text{-OTi(OR')}_3]$  ( $\text{OR}' = \text{OMe}$ ,  $\text{OPr}^i$  and  $\text{BINOL-H}_2 = 1,1'\text{-bi-2-naphthol}$ ). Establishing the catalytic performances of the Ti silsesquioxane model of open lattice sites was complicated by solution dimerization equilibria of the silsesquioxanes [59,60]. UV studies have shown that the monomeric form (i.e. the form most susceptible to be a close molecular analogue to the

**Table 1**  
Structure and Ti–O distances in silica-grafted Ti(IV) trisiloxy and corresponding silsesquioxane models.

Titanium coordination number	Structures		Molecular silsesquioxane	
	Surface silica-grafted species			
	Geometry	Ti–O distances (Å) <sup>a</sup>	Geometry	Ti–O distances (Å) <sup>b</sup>
4		1.81		1.84(2), 1.658(6)
		1.81 2.35		1.837(1), 2.0022(1), 2.004(1), 2.210(1)

<sup>a</sup> Measured by EXAFS.

<sup>b</sup> Measured by X-ray diffraction on single crystals.

<sup>c</sup> Only half-dimer shown.

heterogeneous catalyst surface species) is substantially present in solution, especially for freshly prepared samples, therefore allowing parallels between homogeneous and heterogeneous catalytic performances for the tetrahedrally coordinated Ti(IV) centers discussed here.

The steric congestion can be induced by the Ti ancillary ligands ( $\text{OMe} > \text{OPr}^i > \text{BINOL}$ ) and by the silsesquioxanes cage itself through the interaction with adjacent  $\text{OSiMe}_3$  groups present in **2b** and **1b** and not in **1c** [62]. Overall, out of all the molecular models, the most active, with an activity similar to the surface species appears to be the less sterically encumbered tripodally attached species  $[(\text{R}_7\text{Si}_7\text{O}_9-\text{O}_3\text{Ti}(\text{OR}'))_3]$  ( $\text{OR}' = \text{OMe}$  with  $\text{R} = \text{cyclopentyl}$  [57,60,62];  $\text{OR}' = \text{OSiMe}_3$  with  $\text{R} = \text{cyclohexyl}$  [59,61]).

A very elegant study centered on Ti–silsesquioxanes for better comprehension of the activity of silica-supported Ti epoxidation catalysts has relied on the diffuse reflectance UV (DR-UV) analysis of a series of silica and related silsesquioxane models [63]: the heterogeneous systems under investigation were grafted  $\text{Ti}(\text{OPr}^i)_4$  on different amorphous silicas (MCM-41, Aerosil 200, and MERCK 60 with different degrees of silanization) at different Ti loadings; the molecular system studied were Ti(IV) monopodal, dipodal, or tripodal silsesquioxanes. Firstly, the comparison between spectra of the silica-grafted materials and those of the individual silsesquioxanes allowed the assessment of the relative ratios between the different surface species in the heterogeneous catalysts (Fig. 1).

Secondly, the DR-UV study of cyclohexene epoxidation with  $\text{H}_2\text{O}_2$ , indicated that the crucial structural properties of the silica-grafted Ti(IV) center necessary for good catalytic activity appear to be pentacoordination and accessibility [63]. Interesting support effects were highlighted: for example, the tendency of MCM-41 over other non-porous silicas to yield higher concentrations of tetracoordinated relative to the pentacoordinated species, and tripodal over dipodal species. These assignments are consistent with non-spectroscopic surface-science evidence such as the mass-balance analysis of the reaction between  $\text{Ti}(\text{OPr}^i)_4$  and Aerosil 200  $\text{SiO}_{2-200}$  and  $\text{SiO}_{2-500}$  for which a pentacoordinated monopodal  $[(\equiv\text{SiO})\text{Ti}(\text{OPr}^i)(\mu\text{-OPr}^i)_2\text{Ti}(\text{OPr}^i)_3]$  has been proposed [64]. The study also suggested that the heterogeneous catalysts perform differently than their homogeneous analogues: while for Ti–POSS, the bipodal silsesquioxanes lead to less active catalysts with respect to their tripodal analogues, for the solids  $\text{Ti}(\text{OPr}^i)_4/\text{SiO}_{2,x}$  the larger the portion of bipodal sites over the tripodal sites the better the catalytic activity. The use of  $\text{H}_2\text{O}_2$  as oxidant, and not  $t\text{BuOOH}$ , as in the

homogeneous catalyses, and the ensuing difference in decomposition routes, for the oxidants, have been offered as a possible reason for this difference. The silsesquioxane  $[(\text{C-C}_7\text{H}_{13})_7\text{Si}_6\text{O}_{11}]_3[\text{TiOH}]_4$  is the only molecular silsesquioxanes tested with aqueous hydrogen peroxide and it efficiently catalyzes alkene epoxidations [16]. This intriguing thermally robust tetrameric Ti–polyoxotitanate, which is obtained from the tetrasilanol **4a** is not just a model to heterogeneous catalysts but is an efficient epoxidation catalyst in its own right [16].

Steric access appears to be the predominant factor for both heterogeneous and homogeneous catalysts also for the series of silsesquioxanes  $[(\text{C}_5\text{H}_9)_7\text{Si}_7\text{O}_9-\text{O}_3\text{Ti}(\text{O-EPH}_3)]$  ( $\text{E} = \text{Si}, \text{Ge}, \text{and Sn}$ ) [57] which were considered as models of modified heterogeneous titanium catalysts supported on, respectively, straight mesoporous silica, Ge-doped mesoporous silica by pre-treatment with  $\text{GeBu}_4$ , and Sn-doped mesoporous silica by pre-treatment with  $\text{SnBu}_4$  [65]. The dopant effect on the turnover frequency follows the same trend for the silsesquioxanes and the heterogeneous catalysts  $\text{Ti}/\text{MCM-41}$ ,  $\text{Ti}/\text{Ge}/\text{MCM-41}$ , and  $\text{Ti}/\text{Sn}/\text{MCM-41}$ , i.e.  $\text{TOF} = 18$  vs.  $34 \text{ h}^{-1}$  ( $\text{E} = \text{Si}$ );  $52$  vs.  $40 \text{ h}^{-1}$  ( $\text{E} = \text{Ge}$ );  $33$  vs.  $12 \text{ h}^{-1}$  ( $\text{E} = \text{Sn}$ ), respectively [57].

In the context of asymmetric catalysis, Ti–POSS containing the chiral ligand 1R,2S,5R-(–)-menthoxy ligand (MentO) were synthesized from the monosilanol **2b**– $\text{C}_6\text{H}_{11}$  and  $\text{Ti}(\text{OPr}^i)_4$  (Chart 3). The molecular complexes were tested as asymmetric homogeneous catalysts for the epoxidation of cinnamyl alcohol with *tert*-butylhydroperoxide (TBPH) and compared with the heterogeneous catalyst obtained from the grafting of  $[\text{Ti}(\text{OPr}^i)_2(\text{MentO})]_2$  and  $[\text{Ti}(\text{MentO})_4]$  on silanized SBA-15 [66]. The maximum enantioselectivity for the heterogeneous catalyst was 27% which compared only partly with the maximum enantioselectivity obtained from the best homogeneous Ti(MentO)–POSS catalysts, viz. 15%.

### 3.2.2. Titanocene-, zirconocene- and related half-sandwich based polymerization catalysts

Albeit titanocene dichloride grafting on mesoporous MCM-41 silica followed by calcinations of the ensuing  $[(\equiv\text{SiO})_3\text{TiCp}]$  is an alternative route to high-performance academic variants of the industrial titanasilicalite catalyst [53], silica-grafted titanocene and half-sandwich Ti(IV) complexes have been mostly an entry to polymerization catalysts [17,67,68]. Approaches such as grafting  $\text{CpTiCl}_3$  on silica, followed by methylaluminoxane (MAO) activation [68–70], grafting  $\text{Cp}_2\text{TiCl}_2$  on silica or MAO-modified silica

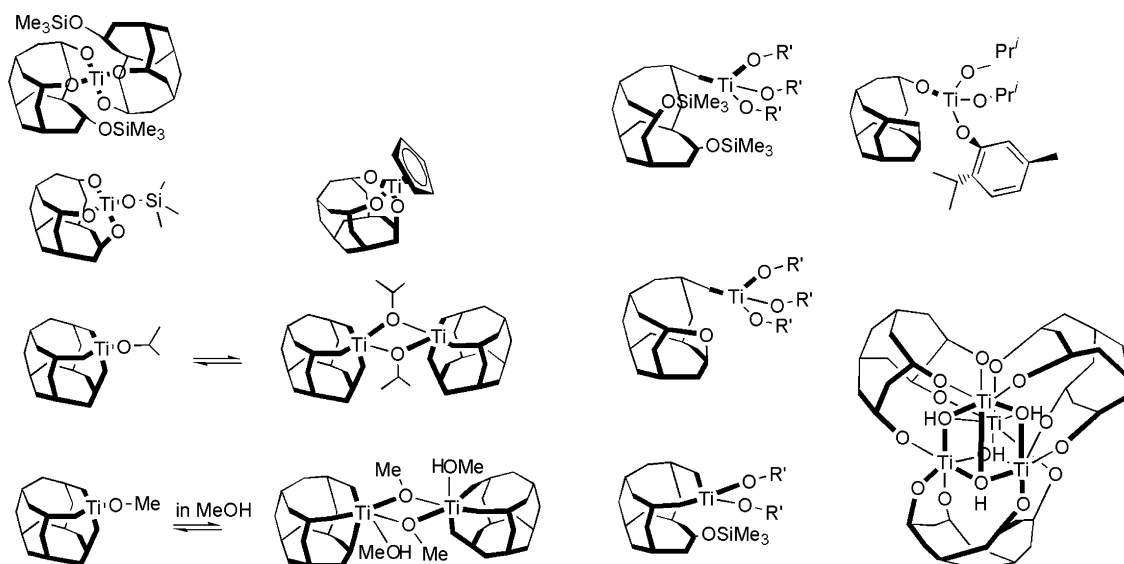
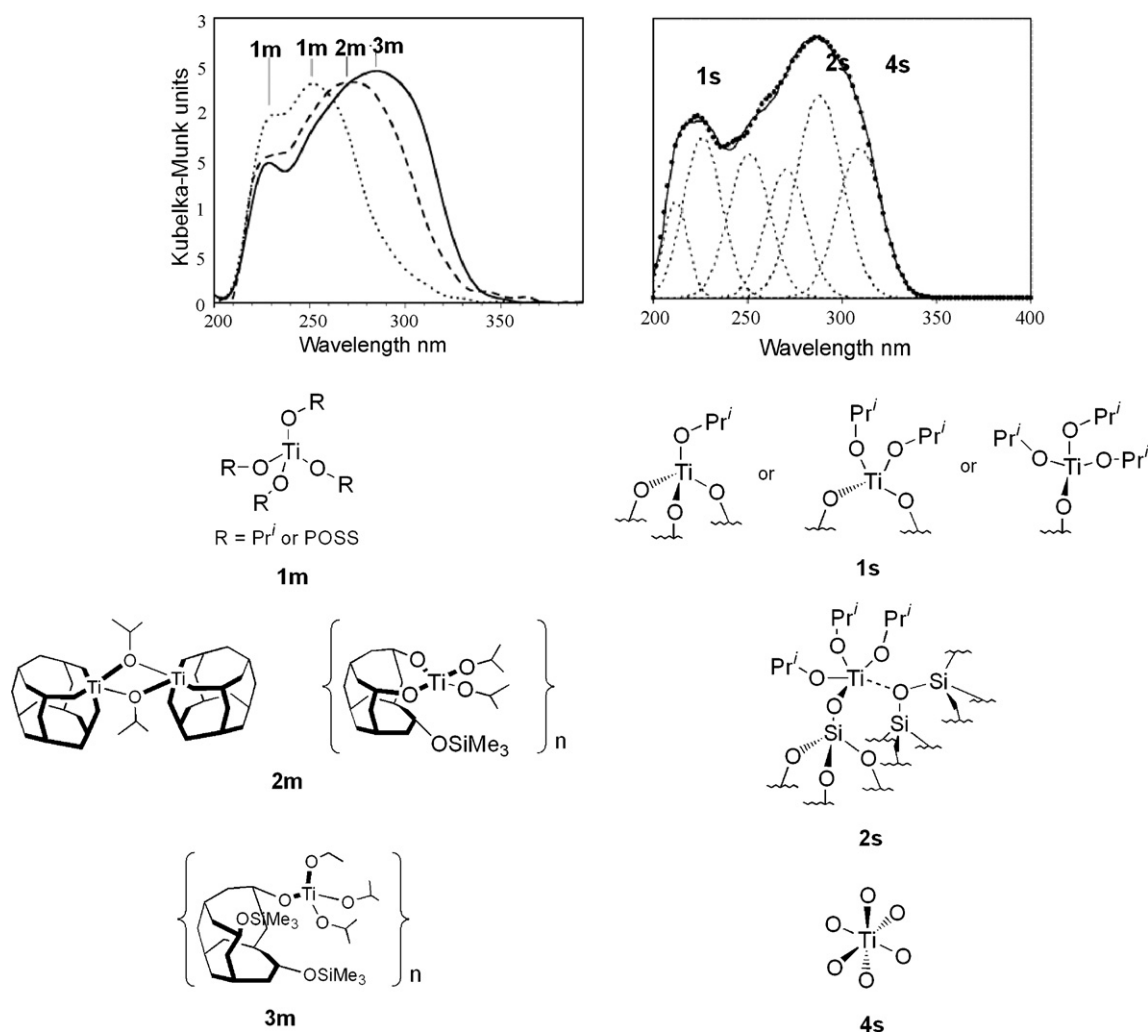


Chart 3. Selected examples of Ti–silsesquioxanes.



**Fig. 1.** (A) DR-UV spectra of Ti-silsesquioxanes complexes with the assigned major species for each maximum. (B) DR-UV spectrum of the  $\text{Ti}(\text{OPri})_4$  grafted on MCM-41 and deconvolution. The fifth ligand in the pentacoordinated species is represented as an adjacent surface siloxane bridge, but water or surface silanols are also possible. Adapted from Ref. [63].

[71] and MCM-41 with MAO as co-catalyst [72], or grafting  $\text{TiCl}_4$  followed by Cp exchange [73] have been reported.

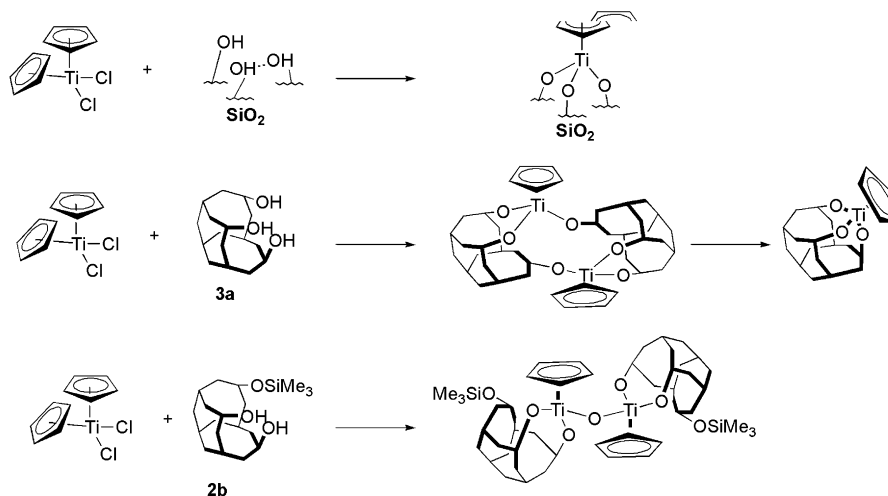
For the unsubstituted titanocene derivatives, the silsesquioxane  $[(\text{C}_6\text{H}_{11})_7\text{Si}_7\text{O}_{12}\text{TiCp}]$ , i.e. an analogue to the organometallic surface species  $[(\equiv\text{SiO})_3\text{TiCp}]$ , can be obtained from either reaction of  $\text{Cp}_2\text{TiCl}_2$  (and  $\text{CpTiCl}_3$ ) with trisilanol **3a**- $\text{C}_6\text{H}_{11}$  [38,74] or by reaction of  $\text{CpTiCl}_3$  with a tris-sibonum derivative of **3a**- $\text{C}_6\text{H}_{11}$  [38] (Scheme 2). The reaction from titanocene dichloride showed the presence of dimers, and more recent work point to the tendency  $\text{Cp}_2\text{TiCl}_2$  and  $\text{Cp}^*\text{TiCl}_2$  to yield  $\mu$ -oxo Ti-POSS derivatives [25,75]. Similarly, decomposition of the metallocene coordination sphere to form inactive surface species has also been reported in a silica-supported system [17]. In solution, the use of a Ti(III) fulvene precursor elegantly circumvented this issue and lead to clean Ti(IV) silsesquioxane [75].

Silsesquioxane models for half-sandwich Ti(IV)-silica derivatives containing 1,3- $\text{C}_5\text{H}_3(\text{SiMe}_3)_2$  ( $\text{Cp}''$ ) bulky cyclopentadienyl ligand were obtained from  $\text{Cp}''_2\text{TiCl}_2$  and monosilanol **1a** [35] and trisilanol **3a** [69]. Both complexes homogeneously catalyze ethylene polymerization in the presence of MAO, and suggest the replacement of at least one Si-O-Ti bond by a Si-O-Al bond, thus hinting at the unstable nature of the heterogeneous catalyst upon addition of the alkylating agent. No evidence for silsesquioxane displacement is observed when activated with  $\text{B}(\text{C}_6\text{F}_5)_3$ ,  $\text{BAR}^{\text{F}_3}$ , as

co-catalyst, rather than with aluminum alkyls and the catalytic activity in ethylene polymerization is retained [35,69]. Addition of a neighbouring siloxane ring in the silsesquioxane cage causes considerable retardation of the polymerization but also improves the catalyst stability, suggesting a parallel with the heterogeneous catalysts for which an interesting surface effect can be invoked [37].

The development of a single-site zirconocene- and half-sandwich zirconium-based heterogeneous catalyst was explored extensively [17,67,76,77]. Direct grafting of  $\text{Cp}_2\text{ZrMe}_2$  or  $\text{Cp}^*\text{ZrMe}_3$  on silica dehydroxylated at or above  $500^\circ\text{C}$ , lead to mostly monografted surface complexes,  $[(\equiv\text{SiO})\text{ZrCp}_2\text{Me}]$  and  $[(\equiv\text{SiO})\text{ZrCp}^*\text{Me}_2]$ , respectively, as indicated by elemental analyses, infrared spectroscopy, and nuclear magnetic resonance ( $^1\text{H}$  and  $^{13}\text{C}$  NMR on enriched compounds) data [78–80]. The grafting reaction of substituted metallocene ( $^{\text{R}}\text{Cp}$ ) $_2\text{ZrCl}_2$  ( $^{\text{R}}\text{Cp} = \text{C}_5\text{H}_4\text{R}$ ,  $\text{R} = \text{H}$ , Me,  $^n\text{Bu}$  and  $^i\text{Bu}$ ), and half-sandwich Zr(IV) chlorides on silica were also extensively studied [71,81,82]. Several molecular models for these inactive surface species have been obtained with silsesquioxanes. Model monografted half-sandwich silsesquioxane Zr(IV)chloro complex containing the disubstituted cyclopentadienyl 1,3- $\text{C}_5\text{H}_3(\text{SiMe}_3)_2$  ( $\text{Cp}''$ ) ligand was synthesized from the reaction of  $\text{Cp}''\text{ZrCl}_3$  with one equivalent of **1a** ( $\text{R} = \text{C}_5\text{H}_9$ ), while addition of a second equivalent of **1a** lead to the structurally characterized bis-siloxy complex  $[(\text{C}_5\text{H}_9)_7\text{Si}_7\text{O}_{12}\text{SiO}]_2\text{ZrClCp}''$ , a potential





**Scheme 2.** Silsesquioxane models for half-sandwich Ti(IV)–silica complex  $[(\equiv\text{SiO})_3\text{TiCp}]$ .

model for the bisgrafted surface species [69]. Silsesquioxane models for a surface trisgrafted species are  $[(\text{C}_6\text{H}_{11})_7\text{Si}_7\text{O}_{12}\text{ZrCp}^*]$  and  $[(\text{C}_6\text{H}_{11})_7\text{Si}_7\text{O}_{12}\text{ZrCp}^*]$  and are obtained, respectively, from reaction of starting **3a**– $\text{C}_6\text{H}_{11}$  with  $\text{Cp}^*\text{ZrMe}_3$  [69] and  $\text{Cp}^*\text{Zr}(\text{CH}_2\text{C}_6\text{H}_5)_3$  [83]. Molecular models for alkyl half-sandwich species are available with trisphenyl silanol as siloxy ligand  $(\text{Ph}_3\text{SiO})\text{ZrCp}^*(\text{CH}_2\text{C}_6\text{H}_5)_2$  and  $(\text{Ph}_3\text{SiO})_2\text{ZrCp}^*(\text{CH}_2\text{C}_6\text{H}_5)$  [69]. Structural distances such as Si–O–Zr bond can be inferred by EXFAS studies at Zr *K*-edge [82] and correlate with molecular data ( $d_{\text{Zr-O}} = 1.9_{\text{silica}} \text{ \AA}$  vs.  $1.985_{\text{silsesquioxane}} \text{ \AA}$ ) [83]. These neutral species, as expected due to the lack of free coordination site on the metal and/or Metal–alkyl bond, are inactive as polymerization catalysts.

Addition of a Lewis acid to the previously mentioned silica-grafted neutral metal alkyls is a well-described successful route to obtain an active polymerization catalyst [17]. Well-defined zirconium surface systems have been obtained by addition of  $\text{BAr}^{\text{F}}_3$  to the surface complex  $[(\equiv\text{SiO})\text{ZrCp}^*\text{Me}_2]$  [80]. The borane addition gives the cationic surface species  $[(\equiv\text{SiO})\text{ZrCp}^*\text{Me}][\text{BAr}^{\text{F}}_3\text{Me}]$ , which further evolves, by methyl transfer on an adjacent siloxane bridge, to  $[(\equiv\text{SiO})_2\text{ZrCp}^*][\text{BAr}^{\text{F}}_3\text{Me}][\equiv\text{SiO-Me}]$ , to yield a ca. 1:2 mixture of monosiloxy and disiloxy cationic species (Scheme 3) [80]. The former is active in polymerization, the latter, which is also the major surface species, is inefficient. Among the molecular models for this system are the benzyl silsesquioxane derivative  $[(\text{C}_5\text{H}_9)_7\text{Si}_7\text{O}_{12}\text{ZrBz}]_2$  (which is a sluggish polymerization catalyst by itself probably due to the involvement of zwitterionic form  $[(\text{C}_5\text{H}_9)_7\text{Si}_7\text{O}_9(\text{O}_3\text{Zr}^-(\mu-\text{O})(\text{BzZr}^+(\text{O}_2(\text{O}_9\text{Si}_7(\text{C}_5\text{H}_9)_7))] \text{ [84] the triphenylsiloxy monocyclopentadienyl complex  $(\text{Ph}_3\text{SiO})_2\text{ZrCp}^*\text{Bz}$  ( $\text{Bz} = \text{CH}_2\text{C}_6\text{H}_5$ ), and the non-metallocene starting peralkyl benzyl complex  $\text{ZrBz}_4$  [78,85]. All become active in ethylene polymerization upon  $\text{BAr}^{\text{F}}_3$  addition (Scheme 3).$

An alternative strategy to synthesize an active polymerization catalyst is to graft the co-catalyst on the surface before the addition of the organometallic precatalysts [17]. This is the usual procedure in industrial metallocene chemistry. Several aluminosilsesquioxanes have been synthesized [25] and have some pertinence to this approach but the overall relevance is limited in the context of floating polymerization catalysts [17]. A more successful route to understanding heterogeneous floating Zr(IV) cationic metallocene consists of the use of organoborane modified silicas by pre-treatment with  $\text{BAr}^{\text{F}}_3$ , possibly in the presence of  $\text{Et}_2\text{NH}$  [86]; and will be discussed in Section 3.11.1 on boron-containing silsesquioxanes.

The tethering approach, or supported homogeneous catalysis, which consists of chemically bonding the surface reactive moiety

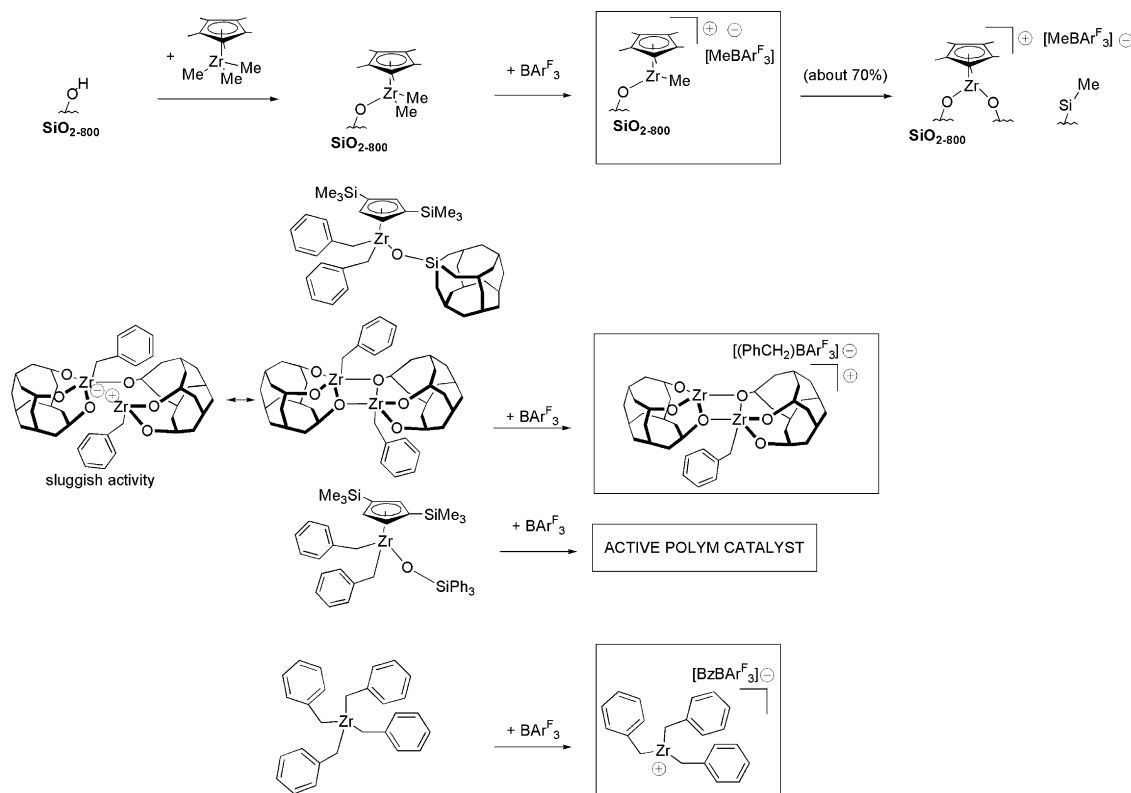
(i.e.  $[\equiv\text{SiOH}]$  for silica) with one end of an organic linker (tether) while coordinating the other end to the active organometallic catalytic center, has been extensively applied toward the development of Zr-based polymerization catalysts [17]. Silsesquioxanes have been successfully applied to model such catalysts without direct metal–surface bond and thus beyond the scope of this review [15,87].

### 3.2.3. Ziegler–Natta type polymerization catalysts

The archetypical heterogeneous catalyst for olefin polymerization is the Ziegler–Natta system(s). While, the catalysts were originally typically obtained by treating crystalline  $\alpha\text{-TiCl}_3$  with  $[\text{AlCl}(\text{C}_2\text{H}_5)_2]_2$ , the most common support is now  $\text{MgCl}_2$  associated with several Lewis base ligands [67,88]. Several surface-science techniques have been applied to the  $\text{TiCl}_4/\text{MgCl}_2/\text{modifiers}$  heterogeneous systems and have demonstrated, *inter alia*, that (i) Ti(III) and Ti(II) surface species are involved in the activated catalyst and that (ii) the local surface structure of  $\text{MgCl}_2$  determines the isotacticity of the polymer [89]. As far as molecular silsesquioxane-based models are concerned, the closest analogue are Ti(III) silsesquioxanes [75,90], but no comparison has been carried out between the catalytic activities of the homogeneous and heterogeneous systems. In the context of Ziegler–Natta catalysis, silica has also been used as a third component to yield “ternary” precatalyst  $\text{TiCl}_4/\text{Cp}_2\text{Mg}/\text{SiO}_2$  activated by MAO [91]. The heterobimetallic Ti–Mg silsesquioxane  $[(\text{C}_6\text{H}_{11})_7\text{Si}_7\text{O}_{12}\text{MgTiCl}_3]_n$  ( $n=1$  or 2) is reported [92] and has been proposed as a structural possibility for the heterogeneous  $\text{TiCl}_4/\text{MgCl}_2$  catalyst [93], or for the  $\text{TiCl}_4/\text{Cp}_2\text{Mg}/\text{SiO}_2$  one (Chart 4). Compound  $[(\text{C}_6\text{H}_{11})_7\text{Si}_7\text{O}_{12}\text{MgTiCl}_3]_n$  catalyses ethylene polymerization in the presence of triethylaluminum co-catalyst. Its activity (of about 111 kg PE/g<sub>Ti</sub> h) and the characteristic of the polymer ( $M_w = 140,000$ ;  $M_w/M_n = 5.5$ ,  $MI = 1.02$ ) are comparable to those of a typical commercial Ti/Mg/SiO<sub>2</sub> silica-supported catalyst [92].

### 3.2.4. Group 4 alkyls and hydrides ( $M = \text{Zr}, \text{Ti}, \text{Hf}$ ) for catalytic hydrocarbon transformations

Silica-supported titanium alkyls can be obtained by grafting  $\text{Ti}(\text{CH}_2\text{CMe}_3)_4$  on silica aerosol  $\text{SiO}_{2-500}$  and on MCM-41<sub>500</sub>: the dominant surface species are  $[(\equiv\text{SiO})\text{Ti}(\text{CH}_2\text{CMe}_3)_3]$  for the former and a mixture of  $[(\equiv\text{SiO})\text{Ti}(\text{CH}_2\text{CMe}_3)_3]$  and  $[(\equiv\text{SiO})_2\text{Ti}(\text{CH}_2\text{CMe}_3)_2]$  for the latter, based on IR spectroscopy, solid-state NMR, XAFS, and elemental analyses data [94]. The titanium silsesquioxane compounds  $[\text{R}_7\text{Si}_7\text{O}_{12}\text{Ti}(\text{CH}_2\text{C}_6\text{H}_5)]$  ( $\text{R} = \text{C}_6\text{H}_{11}$  [59], and  $\text{R} = \text{C}_5\text{H}_9$  [84]) are close structural models for the monografted surface species.



**Scheme 3.** Cationic half-sandwich Zr(IV) surface species obtained from  $\text{BArf}_3$  addition to  $\text{Cp}^*\text{ZrMe}_3$  grafted on silica, and possible silsesquioxane and other molecular models.

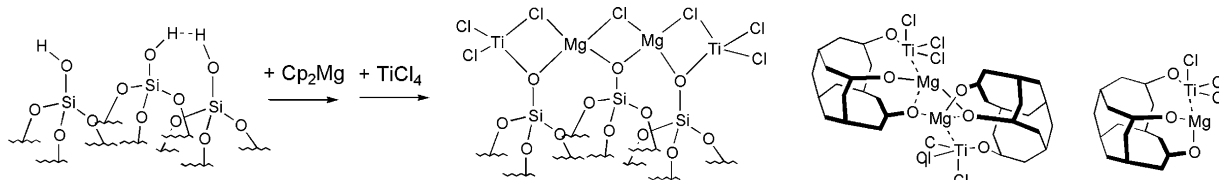
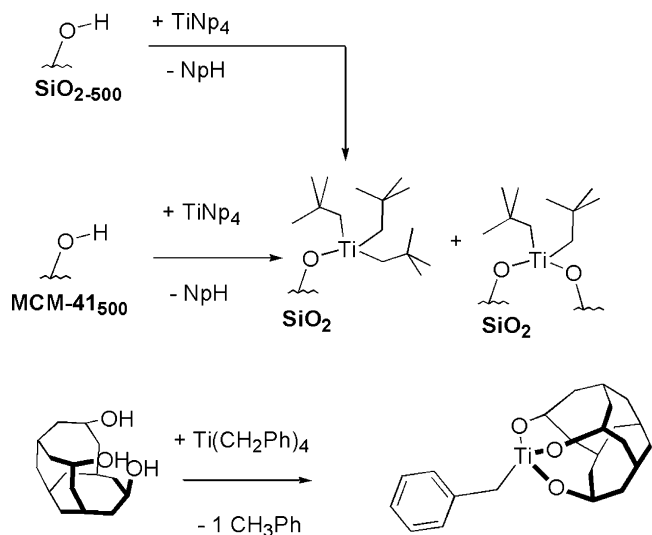


**Chart 4.** Patented route to heterogeneous precatalyst  $\text{TiCl}_4/\text{MgCl}_2/\text{SiO}_2$  with one of the proposed surface structures drawn and possible heterobimetallic Ti–Mg silsesquioxane models.

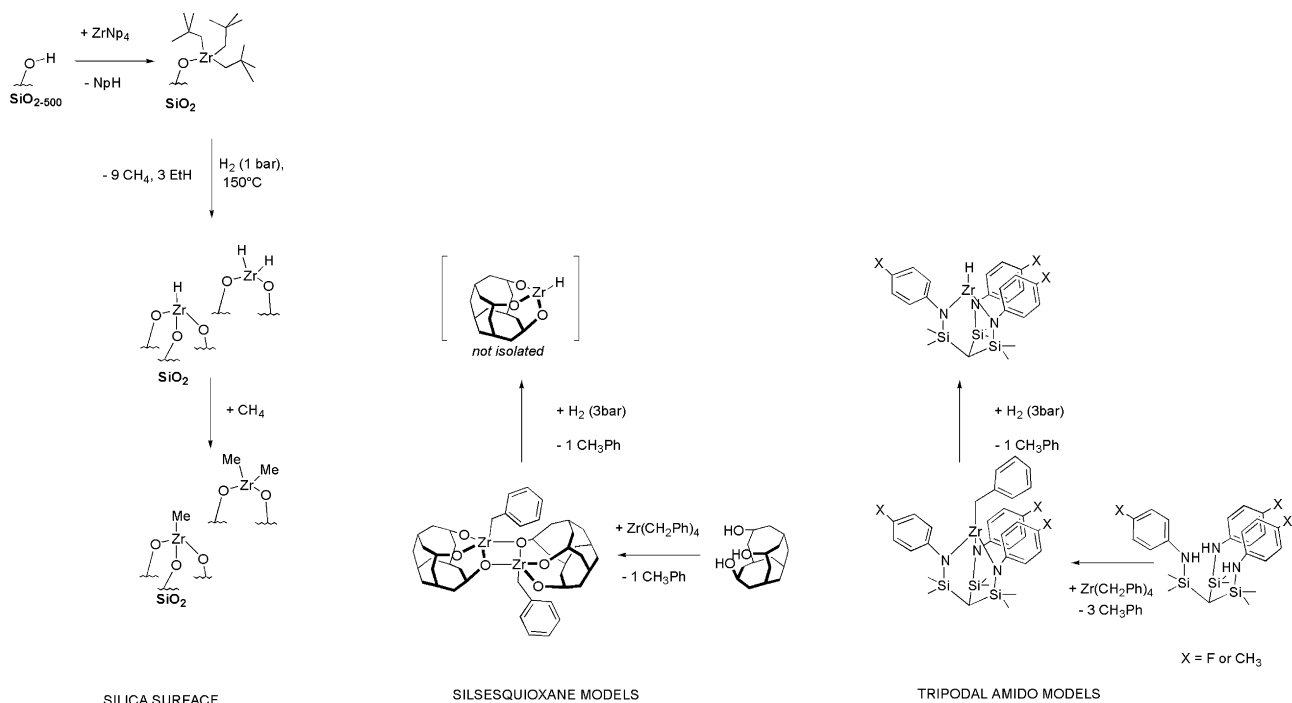


**Scheme 4.** Ti(IV) alkyl surface species (left) and model silsesquioxane analogue (right), displaying formally unusual 8-electron count even in solution.

NMR data show that these Ti-complexes (unlike their Zr and Hf homologues, *vide infra*) are indeed monomeric, yielding a surprising formal 8-electron count even in solution (Scheme 4).

Reactivity-wise, surface studies have shown that  $[(\equiv\text{SiO})\text{Ti}(\text{CH}_2\text{CMe}_3)_3]$  reacts cleanly with alcohol to yield  $[(\equiv\text{SiO})\text{Ti}(\text{OCH}_2\text{CMe}_3)_3]$  [94]; the Ti-monoalkyl silsesquioxane complex proved active as a precursor for homogeneous catalytic olefin epoxidation [59], while the Ti-alkyls *per se* have not been reported in catalytic hydrocarbon transformations.

Three routes are reported to silica-supported Zr(IV) alkyls: (i) by grafting an organometallic precursor on a silica surface (such as, for example  $\text{Zr}(\text{CH}_2\text{CMe}_3)_4$  [95] on silica dehydroxylated at  $500^\circ\text{C}$ ,  $\text{SiO}_{2-500}$ , to give  $[(\equiv\text{SiO})_2\text{Zr}(\text{CH}_2\text{CMe}_3)_2]$  and  $[(\equiv\text{SiO})\text{Zr}(\text{CH}_2\text{CMe}_3)_3]$ ); (ii) by stoichiometric reaction of zirconium hydrides  $[(\equiv\text{SiO})_2\text{ZrH}_2]$  and  $[(\equiv\text{SiO})_3\text{ZrH}]$  [96,97] with an alkane (such as methane [98] – to give  $[(\equiv\text{SiO})_2\text{ZrMe}_2]$  and  $[(\equiv\text{SiO})_3\text{ZrMe}]$  – or cyclooctane [99] to give the cyclooctyl derivative); and (iii) as resting state of the catalyst during the catalytic transformation of hydrocarbons by  $[(\equiv\text{SiO})_2\text{ZrH}_2]$  and  $[(\equiv\text{SiO})_3\text{ZrH}]$  (as for example isomerisation and hydrogenation of long chain polyolefins [100], hydrogenolysis of alkanes [101,102], Ziegler–Natta type depolymerization [103], etc.). A silsesquioxane model for the trisgrafted surface species  $[(\equiv\text{SiO})_3\text{ZrMe}]$  is obtained by reaction of  $\text{Zr}(\text{CH}_2\text{Ph})_4$  with trisilanol **3a** ( $\text{R} = \text{C}_5\text{H}_9$ )

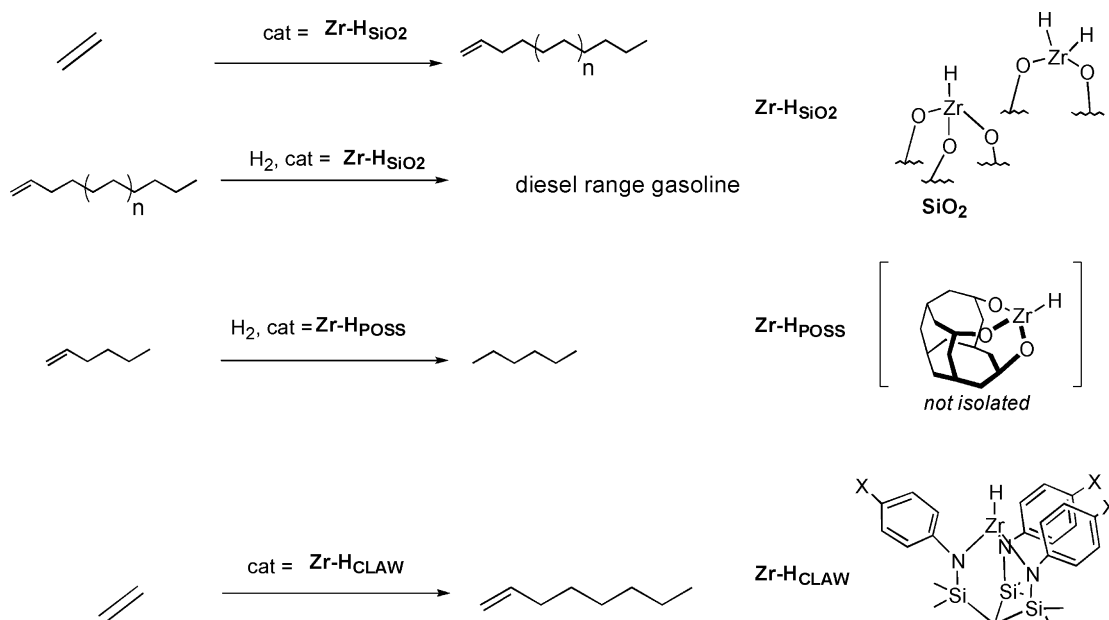


**Scheme 5.** Zr(IV) alkyl surface species (left) and model silsesquioxane (center) and tripodal amido models (right), most of them displaying formally unusual 8-electron count.

to yield  $[(\text{C}_5\text{H}_9)_7\text{Si}_7\text{O}_{12}\text{Zr}(\text{CH}_2\text{Ph})]_2$  which has been structurally characterized in the solid state (Scheme 5). Reaction of the same Zr(IV) tetrabenzyl precursor (or of related  $\text{ZrCl}_2(\text{CH}_2\text{Ph})_2 \cdot 2\text{THF}$ ) with disilanol silsesquioxane **2b**- $\text{C}_5\text{H}_9$ ,  $\text{R}' = \text{OSiMe}_3$ ) fails to give a model for the bipodal surface dialkyl species since it yields alkyl-free bis-silsesquioxane derivatives  $[(\text{C}_5\text{H}_9)_7\text{Si}_7\text{O}_{11}(\text{OSiMe}_3)]_2\text{Zr}$  (and  $[(\text{C}_5\text{H}_9)_7\text{Si}_7\text{O}_{11}(\text{OSiMe}_3)]_2\text{Zr}(\text{THF})_2$ ) [84]. An attempt to isolate a POSS–zirconium(IV) hydride by hydrogenating  $[(\text{C}_5\text{H}_9)_7\text{Si}_7\text{O}_{12}\text{Zr}(\text{CH}_2\text{Ph})]_2$ , in order to obtain a close model for surface species  $[(\equiv\text{SiO})_3\text{ZrH}]$  was met by partial success, but isolation of toluene, the expected side product of the hydrogenation, and activity of the ensuing solution toward catalytic hydrogenation

of 1-hexene hints at the possible formation of such hydride (Schemes 5 and 6). Use of the tripodal triamido claw complex  $\text{CH}[\text{Me}_2\text{SiNH}(\text{C}_6\text{H}_5\text{X})]_3$  (X = F and Me as a molecular model for a tripodal grafting site) [9] proved a better approach since the monohydride could be synthesized, observed spectroscopically in solution under its monomeric form, and crystallographically as a dimer in the solid state (Scheme 5) [104]. The  $^1\text{H}$  NMR of the hydrides compare reasonably well between the molecular and the surface species [ $\delta(\text{Zr-H}) = 8.06 \text{ ppm}$  ( $\text{C}_6\text{D}_6$  solution) [104] and  $10.1 \text{ ppm}$  (MAS SS) [104]].

The trisamido Zr(IV) hydride, and its butyl analogue catalyze polymerization of ethylene [104] by analogy with surface species



**Scheme 6.** Hydrocarbon transformation catalyzed by silica-grafted and molecular Zr(IV) hydrides.

(Scheme 6) [96]. The molecular Zr(IV) hydride also catalyzes the cyclization of 1,5-hexadiene [104].

Silica-supported hafnium mono and bis hydrides [105] and hafnium bis and tris alkyl surface species are reported [106]. They are modelled by silsesquioxane  $[(C_5H_9)_7Si_7O_{12}Hf(CH_2Ph)]_2$  [84], which by analogy with the Zr analogue (*vide supra*) catalyses hydrogenation of 1-hexene, ethylene polymerization. The sluggish rate of the latter reaction is accelerated by addition of  $BAr^F_3$  [84]. Hafnium metallocenes have been grafted on silicas [71] and a comparative study on the metal effect over the activity has been carried out ( $Ti < Hf < Zr$ ). Hafnium containing silsesquioxanes include the half-sandwich species  $[(C_6H_{11})_7Si_7O_{12}HfCp^*]$  [25].

### 3.2.5. Zirconium acetylacetonate as an acrylate trans-esterification catalyst

Silica-supported Zr(IV) acetylacetonate surface complexes  $[(\equiv SiO)_3Zr(acac)]$  and  $[(\equiv SiO)_2Zr(acac)_2]$  ( $acac = MeCOCHCOMe$ ) catalyze the trans-esterification of acrylates [107], for which the corresponding silsesquioxane exhibit excellent catalytic properties (Scheme 7) [1,107,108].

## 3.3. Group 5

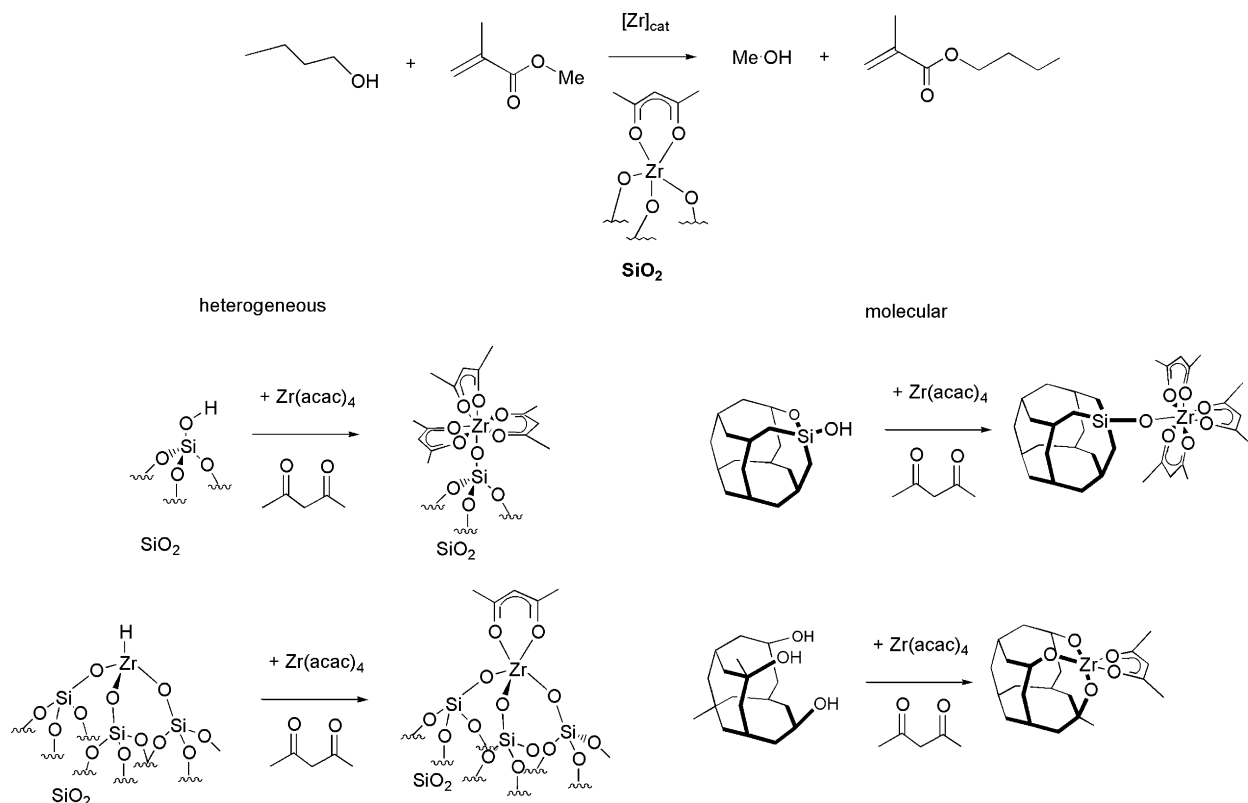
### 3.3.1. Vanadium oxides for selective oxidations

Silica-supported vanadium oxides can catalyze the selective oxidation of  $NO_x$  and hydrocarbons [109,110]. The structure of the catalyst has been assigned as a tetrahedral oxovanadium(V) species such as  $[(\equiv SiO)_3VO]$ , through *inter alia* Raman and  $^{51}V$  NMR data [109], rather than to octahedral coordinated decavanadate-like structures. Silsesquioxane played a crucial role in this structural proposal since they helped the assignment of the original Raman and NMR spectra by comparison of the homologous spectroscopic data acquired on the triphenylsiloxy monomeric and on the silsesquioxanes dimeric analogue of the

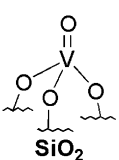
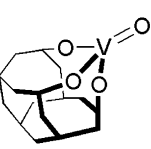
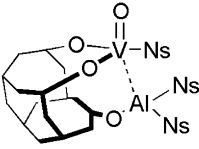
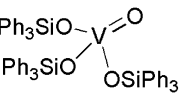
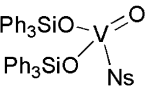
vanadyl moiety,  $(Ph_3SiO)_3V=O$  and  $[(C_6H_{11})_7Si_7O_{12}V=O]_2$ , respectively [109,111,112]. The crystal data for the latter molecule provided accurate structural data for the grafted oxovanadium(V) moiety in the siliceous framework. Novel vibrational [113] and XAFS [114] studies on silica-supported vanadium oxide catalysts further showed that the pyramidal  $[(\equiv SiO)_3VO]$  structure coexists with the umbrella structures  $[(\equiv SiO)_2VO(OH)_2]$  and  $[(\equiv SiO)_2VO(OH)]$ , depending on the hydroxylation degree of the support. Monopodal [115,116] and bipodal [117,118] species were also observed under other impregnation condition and/or with different analytical approaches. The geminal  $[\equiv Si(OH)_2]$  surface species present on  $\beta$ -cristobalite (1 0 0) planes were suggested as possible grafting sites for the bipodal models [118]. Attempts to model such coordination with the geminal silsesquioxane **5b**,  $C_5H_9$  lead to the isolation of the dimer  $[(C_5H_9)_7Si_7O_{10}(OSiMePh_2)-iO_2V=O(OPr^i)]_2$  whose solid-state structure shows that the geminal  $Si(OH)_2$  units do not bind to vanadium oxo units via both siloxide units if vicinal OH are available [119]. The cyclopentyl version of the same silsesquioxane was used as catalyst for the photooxidation of benzene and cyclohexane, and tested well in comparison with the heterogeneous  $V_2O_5/SiO_2$  catalyst [120].

### 3.3.2. Alkylated vanadium oxides for olefin polymerization

Silica-supported vanadium oxides become heterogeneous catalysts for olefin polymerization after activation by MAO [17]. Similarly, vanadium(V) silsesquioxane  $[(C_6H_{11})_7Si_7O_{12}VO]$  [111] becomes a homogeneous catalyst for olefin polymerization when  $AlMe_3$  (1–5 equiv./V) is added to the solution (Chart 5) [112]. The narrow polydispersity of the PE obtained with two equivalents of  $AlMe_3$  ( $M_w/M_n = 2.28$ ) indicates the nearly single-site character of the active species. Careful low-temperature NMR studies with  $AlN_3$  ( $Ns = CH_2SiMe_3$ , neosilyl) as alkylating agent have shown stepwise neosilyl transfer from



Scheme 7. Silica-grafted trans-esterification catalysts and silsesquioxane-based models.

Inorganic precursor	Alkylated catalyst	activity as $\alpha$ -olefin polymerization catalyst
 SiO <sub>2</sub>	$\xrightarrow{+ \text{MAO}}$ [ ill-defined active heterogeneous catalyst ]	YES
	$\xrightarrow{+ \text{Ns}_3\text{Al}}$ 	YES
	$\xrightarrow{+ \text{Ns}_3\text{Al}}$ -no reaction- 	NO
		YES

**Chart 5.** The activation of V-based silica-supported polymerization catalyst with alkylating agent MAO can be modelled with AlNs<sub>3</sub> on silsesquioxane model and not on the triphenylsilanol one.

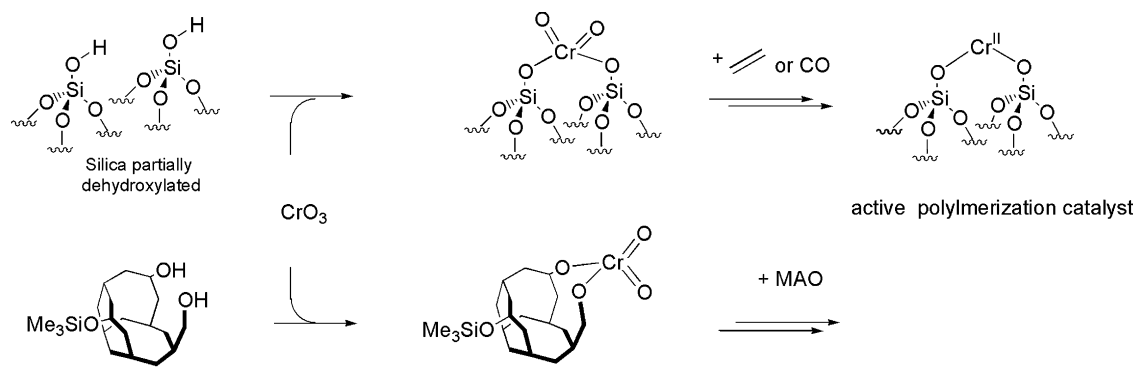
the alkylating aluminum species to the vanadium center. The product [(C<sub>6</sub>H<sub>11</sub>)<sub>7</sub>Si<sub>7</sub>O<sub>9</sub>(OAlNs<sub>2</sub>)(O<sub>2</sub>VONS)], which could be the active species in freshly activated solution, slowly evolves to [(C<sub>6</sub>H<sub>11</sub>)<sub>7</sub>Si<sub>7</sub>O<sub>9</sub>(O<sub>2</sub>AlNs)(O<sub>2</sub>VONS)], which also catalyses PE synthesis but with higher polydispersity ( $M_w/M_n = 5.72$ ) [23,121].

The monomer [(C<sub>6</sub>H<sub>11</sub>)<sub>7</sub>Si<sub>7</sub>O<sub>12</sub>VO] is also a good butadiene polymerization catalyst and is a less performing but still active propylene polymerization and copolymerization catalyst. Under similar conditions, (Ph<sub>3</sub>SiO)<sub>3</sub>VO is not a polymerization catalyst upon addition of alkylating agent [122], while preformed mixed alkyl siloxide complexes (Ph<sub>3</sub>SiO)<sub>n</sub>(Me<sub>3</sub>SiCH<sub>2</sub>)<sub>3-n</sub>VO are (Chart 5) [121]. This case exemplifies the superiority of silsesquioxanes over simpler ligands such as triphenyl silanol as model for silica-rafter supported catalyst when surface chemistry such as dimetallic interactions (such as Al...V interactions implied in the alkylation step required for the catalytic activity) are involved.

### 3.4. Group 6

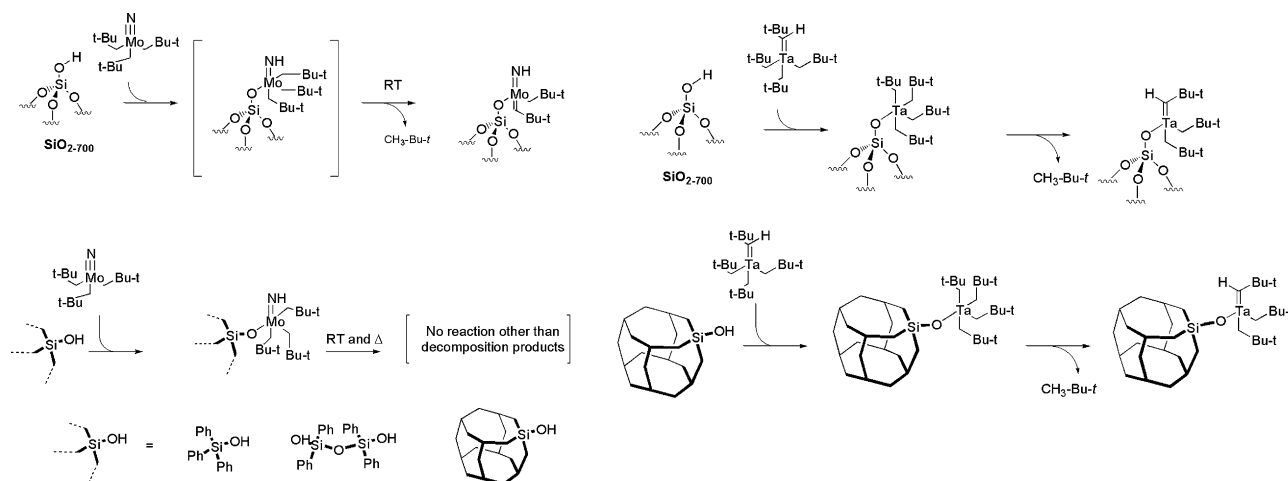
#### 3.4.1. Chromium-based models for polymerization catalysts

Silica-supported Cr(VI) chromate [(=SiO)<sub>2</sub>CrO<sub>2</sub>] is a precursor of the Phillips catalyst for ethylene polymerization [17,31]. The silsesquioxane chromate [(c-C<sub>6</sub>H<sub>11</sub>)<sub>7</sub>Si<sub>7</sub>O<sub>9</sub>(OSiMe<sub>3</sub>)<sub>2</sub>CrO<sub>2</sub>], which can be obtained either from the reaction of CrO<sub>3</sub> with bisilanol **2b**-C<sub>6</sub>H<sub>11</sub> [123], or from reaction of the di-thallated derivative of **2b** with CrO<sub>2</sub>Cl<sub>2</sub> [124], is a molecular model for such silica-supported chromate. The silica-grafted chromate can be activated directly to a very efficient ethylene polymerization heterogeneous catalysts by ethylene itself or by reduction under CO, to yield active Cr(II) bisiloxo species, [(=SiO)<sub>2</sub>Cr] [31]; in contrast, the molecular silsesquioxane analogue does not lead to an active polymerization catalyst under ethylene (albeit only low ethylene pressure were tested); the silsesquioxane chromate requires the



**Scheme 8.** Silica-grafted Phillips catalyst for ethylene polymerization and silsesquioxane model.





**Scheme 9.** Analogies and contrasts between surface and molecular reactions to siloxo Mo(VI) and Ta(V) neopentylidene complexes.

addition of methyaluminoxane as co-catalyst to yield an active polymerization catalyst. The comparison between the heterogeneous and homogeneous catalytic systems is therefore possible but suffers from the lack of molecular definition of the active homogeneous species obtained after activation with the alkylating agent (Scheme 8) [123].

### 3.4.2. Molybdenum-oxo dehydrogenation catalysts

Molybdocene dichloride,  $\text{Cp}_2\text{MoCl}_2$ , reacts with silica surface silanols and, after calcination, yields an active catalyst for oxidative dehydrogenation of methanol to formaldehyde [125]. XAS studies indicate that the calcined species contains isolated tetracoordinate Mo(VI) catalytic centers  $[(\equiv\text{SiO})_2\text{MoO}_2]$ , when the initial metal loading is low, viz. 0.6 mol% [125]. Attempts to obtain the silsesquioxane analogue of this latter species by reaction of  $\text{MoO}_2\text{Cl}_2$  with the bis tetramethyl stibonium derivative of **2b**- $\text{C}_5\text{H}_9$  failed because the POSS cyclocondensed and produced untractable mixtures of molybdate salts,  $[\text{MoCl}_2\text{O}_2]^{2-}$  [38]. Reaction of  $\text{MoO}_2\text{Cl}_2$  with the bis-thallium derivative of **2b**- $\text{C}_6\text{H}_{11}$  and **2b**- $\text{C}_5\text{H}_9$  gave the desired model  $[\text{R}_7\text{Si}_7\text{O}_9(\text{OSiMe}_3)-\text{O}_2\text{MoO}_2]$  [124].

### 3.4.3. Molybdenum and tungsten imido carbene as olefin metathesis catalysts

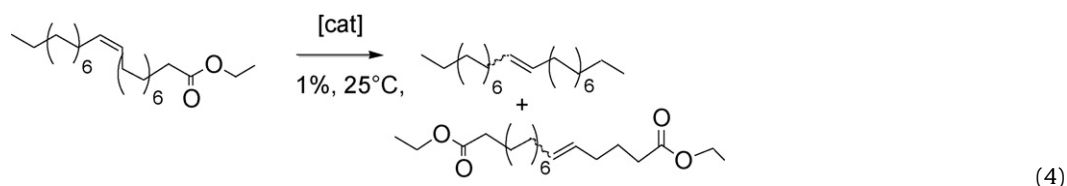
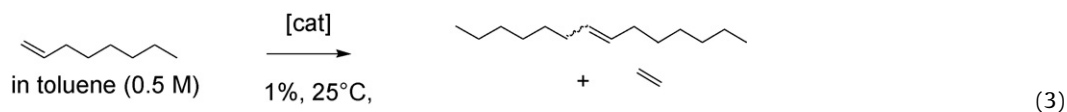
The silica-grafted Mo(VI) complex  $[(\equiv\text{SiO})\text{Mo}(=\text{CH}-t\text{Bu})(-\text{CH}_2-t\text{Bu})(=\text{NH})]$ , obtained from grafting trisneopentyl Mo(VI) nitride,  $\text{Mo}(-\text{CH}_2-t\text{Bu})_3(=\text{N})$ , on silica followed by reductive elimination of neopentane [126,127], is an active olefin metathesis catalyst [128]. Molecular models of the expected trisneopentyl intermediate

$t\text{Bu}_3(=\text{NH})_2$ , and  $[(c-\text{C}_5\text{H}_9)_7\text{Si}_7\text{O}_{12}\text{SiOMo}(-\text{CH}_2-t\text{Bu})_3(=\text{NH})]$  [127]. In contrast with surface chemistry, and with Ta-analogues [129–131], further evolution of the perneopentyl molecular complexes to a neopentylidene derivative is not observed in solution by thermal activation (Scheme 9), and has been observed only if trimethylphosphine is added to the silsesquioxane derivative [127].

The surface Mo(VI) imido carbene  $[(\equiv\text{SiO})\text{Mo}(=\text{CH}-t\text{Bu})(-\text{CH}_2-t\text{Bu})(=\text{NH})]$  is an active catalyst toward propene metathesis (780 equiv.,  $\text{TOF}_{5\text{min}} = 0.89 \text{ mol}_{\text{propene}}/\text{mol}_{\text{Mo}} \text{ s}$  for the catalyst obtained by benzene impregnation route) and ethylene (100 equiv.;  $\text{TOF}_{5\text{min}} = 0.11 \text{ mol}_{\text{oleate}}/\text{mol}_{\text{Mo}} \text{ s}$  for the catalyst obtained by benzene impregnation route) [127]. The high catalytic activity of the surface neopentylidene complex has not been modelled by the silsesquioxane analogue [127].

Grafting on silica dehydroxylated at  $700^\circ\text{C}$  of  $[\text{Mo}(=\text{N}-\text{C}_6\text{H}_3^i\text{Pr}_2)(=\text{CH}-t\text{Bu})(-\text{CH}_2-t\text{Bu})_2]$ , rather than the aforementioned nitride complex, yielded the novel Mo(VI) imido surface complex  $[(\equiv\text{SiO})\text{Mo}(=\text{CH}-t\text{Bu})(-\text{CH}_2-t\text{Bu})(=\text{N}-\text{C}_6\text{H}_3^i\text{Pr}_2)]$  which has been very closely modelled by the silsesquioxane analogue  $[(c-\text{C}_5\text{H}_9)_7\text{Si}_7\text{O}_{12}\text{SiO}-\text{Mo}(=\text{CH}-t\text{Bu})(-\text{CH}_2-t\text{Bu})(=\text{N}-\text{C}_6\text{H}_3^i\text{Pr}_2)]$  and the tetrasiloxo complex  $[(t\text{BuO})_3\text{SiO}-\text{Mo}(=\text{CH}-t\text{Bu})(-\text{CH}_2-t\text{Bu})(=\text{N}-\text{C}_6\text{H}_3^i\text{Pr}_2)]$  [132]. The latter, analyzed by X-ray diffraction study on a single crystal, allowed one to observe the expected *syn* isomer. The molecular and the surface species displayed very similar NMR resonances.

The starting organometallic precursor, the silica-supported species and the silsesquioxane complexes are active catalysts for *n*-oct-1-ene and ethylene self-metathesis reactions (reactions (3) and (4), respectively):

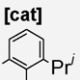
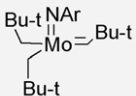
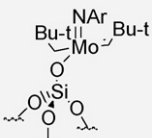
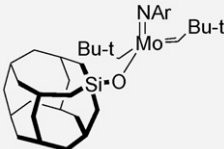
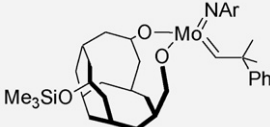


are obtained by reaction of the nitride precursor with either trisphenylsilanol [128], disiloxy complex  $\text{Ph}_2(\text{SiOH})-\text{O}-\text{Ph}_2\text{SiOH}$  [128], or the monosilanol silsesquioxane **1a**- $\text{C}_5\text{H}_9$  [127], to yield, respectively  $[(\text{Ph}_3\text{SiO})\text{Mo}(-\text{CH}_2-t\text{Bu})_3(=\text{NH})]$ ,  $\text{O}[(\text{Ph}_2\text{SiO})\text{Mo}(-\text{CH}_2-$

While the initial TOFs are very similar for the heterogeneous and the homogeneous siloxy catalysts (Table 2), and far better than the starting organometallic complex (hence showing the enhancing catalytic effect of the siloxy moiety), the homogeneous silsesquiox-

**Table 2**

TOF and time necessary to reach equilibrium for octene and ethyloleate self-metathesis reactions (reactions (3) and (4)) by silica-supported, silsesquioxane, and molecular Mo(VI) precursor catalysts. Refs. [127,133].

Ar = 	TOF <sub>5 min</sub> for reaction (3) (time necessary to reach equilibrium)	TOF <sub>5 min</sub> for reaction (4) (time necessary to reach equilibrium)
	0.02 mol <sub>octene</sub> /mol <sub>Mo</sub> s (–[48 h to reach 40% conv. rather than 50%])	0.03 mol <sub>oleate</sub> /mol <sub>Mo</sub> s (–[deactivation after 2% conv.])
	0.06 mol <sub>octene</sub> /mol <sub>Mo</sub> s (10 min)	0.04 mol <sub>oleate</sub> /mol <sub>Mo</sub> s (60 min)
	0.06 mol <sub>octene</sub> /mol <sub>Mo</sub> s (60 min)	0.03 mol <sub>oleate</sub> /mol <sub>Mo</sub> s (24 h)
	7 mol <sub>octene</sub> /mol <sub>Mo</sub> s <sup>a</sup> (120 min)	(120 min)

<sup>a</sup> In neat 1-octene, ca. 3%cat, TOF calculated after 20 s.

ane system deactivated much faster than the heterogeneous one (presumably by bimolecular pathways unavailable to the silica-supported catalysts) [132], thus showing the advantage of sturdy site isolation obtained on the silica-supported catalyst over solution chemistry of homogeneous catalysts, *ceteris paribus*.

The similar silsesquioxane derivative [(c-C<sub>6</sub>H<sub>11</sub>)<sub>7</sub>Si<sub>7</sub>O<sub>9</sub>(OSiMe<sub>3</sub>)<sub>2</sub>O<sub>2</sub>Mo(=CH-CMe<sub>2</sub>Ph)(=N-C<sub>6</sub>H<sub>3</sub><sup>i</sup>Pr<sub>2</sub>)] [133] is also an active olefin metathesis (activity reported toward 1-octene, cis-2-octene, and methyl oleate) [133], with an activity comparable to its organometallic precursor, [(CF<sub>3</sub>)<sub>2</sub>MeC(O)<sub>2</sub>Mo(=CH-CMe<sub>2</sub>Ph)(=N-C<sub>6</sub>H<sub>3</sub><sup>i</sup>Pr<sub>2</sub>)]. No direct comparison with silica-supported bisgrafted analogue is available.

The reaction of [W(=Ar)(=CH<sup>t</sup>Bu)(CH<sub>2</sub><sup>t</sup>Bu)<sub>2</sub>] (Ar = 2,6-<sup>i</sup>PrC<sub>6</sub>H<sub>3</sub>) with a silica partially dehydroxylated at 700 °C, SiO<sub>2</sub>-700, gives *syn*-[(=SiO)W(=NAr)(=CH<sup>t</sup>Bu)(CH<sub>2</sub><sup>t</sup>Bu)] as the major surface species, which was fully characterized by mass-balance analysis, IR, NMR, EXAFS, and modelled theoretically with DFT periodic calculations [134], and molecularly with **1a**-C<sub>5</sub>H<sub>9</sub> (R = C<sub>5</sub>H<sub>9</sub>) to give [(C<sub>5</sub>H<sub>9</sub>)<sub>7</sub>Si<sub>7</sub>O<sub>12</sub>SiO)W(=NAr)(=CH<sup>t</sup>Bu)(CH<sub>2</sub><sup>t</sup>Bu)] [134]. Surface and molecular model display striking similarities as shown for example by the common low *J*<sub>C-H</sub> coupling constants for both alkylidene signals in the NMR spectra (*J*<sub>C-H</sub> = 107 Hz for <sup>13</sup>C solution spectra of the silsesquioxanes vs. *J*<sub>C-H</sub> = 107 Hz for *J*-resolved 2D <sup>1</sup>H–<sup>13</sup>C HETCOR solid-state MAS NMR spectrum of the <sup>13</sup>C labelled for the silica-grafted compound) [134].

When the same organometallic W(VI) precursor [W(=Ar)(=CH<sup>t</sup>Bu)(CH<sub>2</sub><sup>t</sup>Bu)<sub>2</sub>] is reacted with silica partially dehydroxylated at 200 °C, rather than at 700 °C, which has higher concentration of surface silanols, and thus larger probability to yield bisgrafted species, surface species [(=SiO)<sub>2</sub>W(=NAr)(=CH<sup>t</sup>Bu)(CH<sub>2</sub><sup>t</sup>Bu)], [(=SiO)<sub>2</sub>W(=NAr)(CH<sub>2</sub><sup>t</sup>Bu)<sub>2</sub>] and *syn*-[(=SiO)W(=NAr)(=CH<sup>t</sup>Bu)(CH<sub>2</sub><sup>t</sup>Bu)], are obtained [135]. All species were characterized by infrared spectroscopy, 1D and 2D solid-state MAS NMR, elemental analysis and molecular models

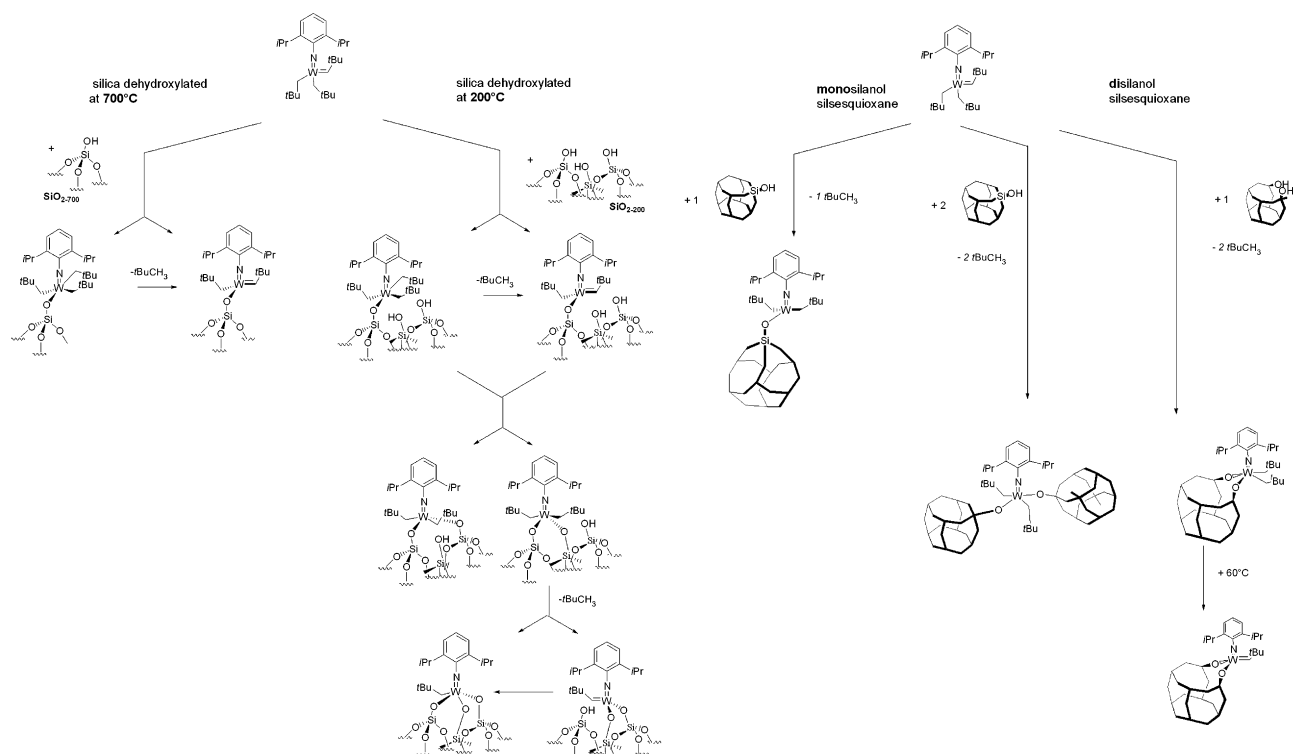
obtained by using silsesquioxanes **1a**-C<sub>5</sub>H<sub>9</sub> and **2a**-C<sub>5</sub>H<sub>9</sub> [135]. The silsesquioxanes models for the expected bisgrafted W(VI) surface products were obtained by reaction of the starting W(VI) alkylidene with either two equivalents on monosilanol **1a** or with one equivalent of *endo* silanol **2a** [135]. Both reactions lead to a bisoxo bissalkyl derivative, and only the latter evolved to an alkylidene upon gentle thermal treatment. This alkylidene was identified as the sole disilsesquioxane species active in olefin metathesis. Comparison of NMR data between these molecules (solution spectra) and the surface species obtained by the grafting of [W(=Ar)(=CH<sup>t</sup>Bu)(CH<sub>2</sub><sup>t</sup>Bu)<sub>2</sub>] on silica dehydroxylated at 200 °C (solid-state spectra) allowed the proposal of a grafting reaction sequence for the organometallic W(VI) precursor on the silica surface (Scheme 10) [135].

Comparison of the catalyst activities of the (inactive) precursor [W(=Ar)(=CH<sup>t</sup>Bu)(CH<sub>2</sub><sup>t</sup>Bu)<sub>2</sub>], the heterogeneous catalysts obtained by grafting the precursor on SiO<sub>2</sub>-700, SiO<sub>2</sub>-200, and the homogeneous silsesquioxanes-based catalysts showed that the surface complex is a highly active propene metathesis catalyst, which can achieve a TON of 16,000 within 100 h, with only a slow deactivation.

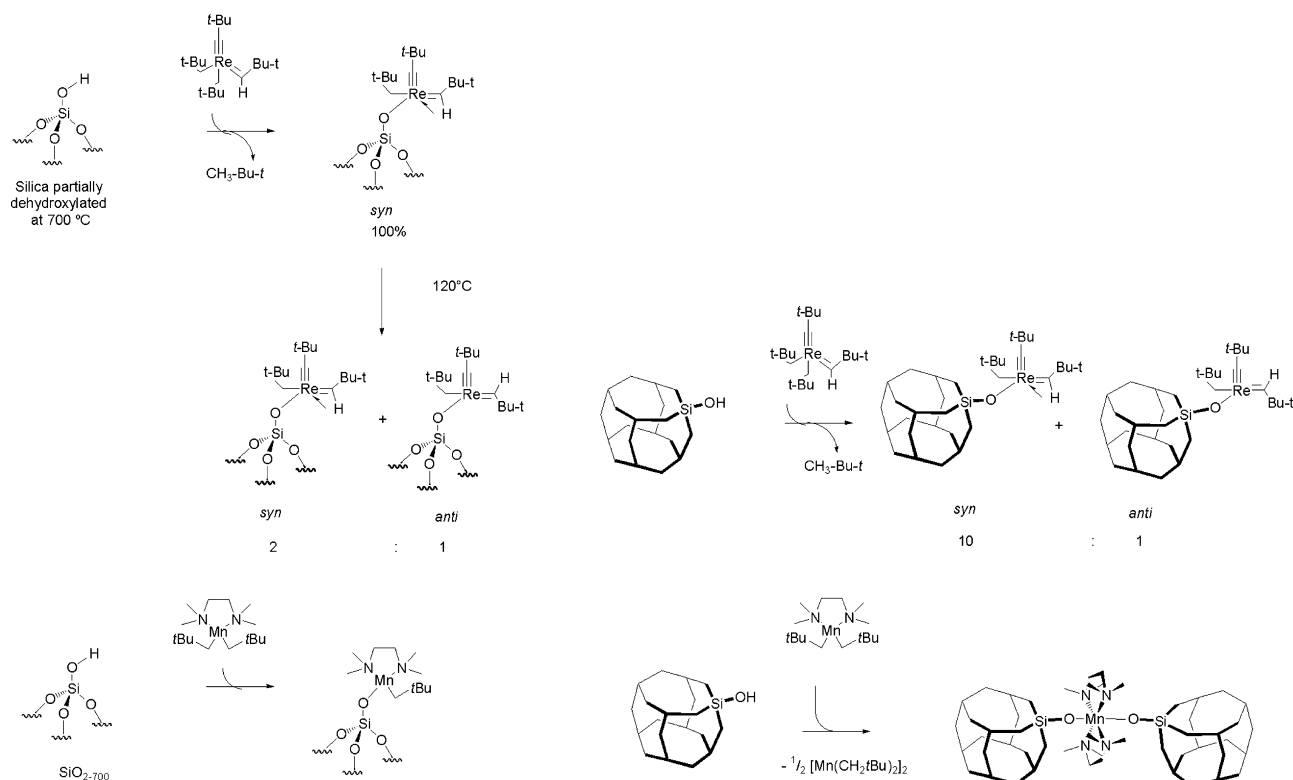
#### 3.4.4. Molybdenum alkylidyne for alkyne metathesis and homodimerization catalyst

The molybdenum(VI) alkylidyne trisamide complex Mo{N-tBu(3,5-C<sub>6</sub>H<sub>3</sub>Me<sub>2</sub>)<sub>3</sub>(=C-Et)}<sub>3</sub> reacts with silica previously dehydroxylated at 400 °C to yield predominantly [(=SiO)Mo(≡C-Et){=N(3,5-C<sub>6</sub>H<sub>3</sub>Me<sub>2</sub>tBu)}<sub>2</sub>], and some [(=SiO)<sub>2</sub>Mo(≡C-Et){=N(3,5-C<sub>6</sub>H<sub>3</sub>Me<sub>2</sub>tBu)}] as shown by elemental analyses and mass-balance studies [136].

The material is an active catalyst for metathesis of a wide spectrum of alkynes and it catalyzes homodimerization of some alkynes while it is inactive in polymerization, thus becoming an interesting alternative to homogeneous analogues that cannot avoid this prob-



**Scheme 10.** Proposed surface reaction scheme for grafting  $[W(=Ar)(=CH^tBu)(CH_2^tBu)_2]$  on silica dehydroxylated at 700 °C vs. silica dehydroxylated at 200 °C (left), obtained through analogy with silsesquioxane chemistry (right).



**Scheme 11.** Analogies and differences between silica surface chemistry and silsesquioxane solution chemistry with group 7  $Re(C-tBu)(=CH-tBu)(-CH_2-tBu)_2$  and  $Mn(-CH_2-tBu)_2(tmeda)$  complexes.

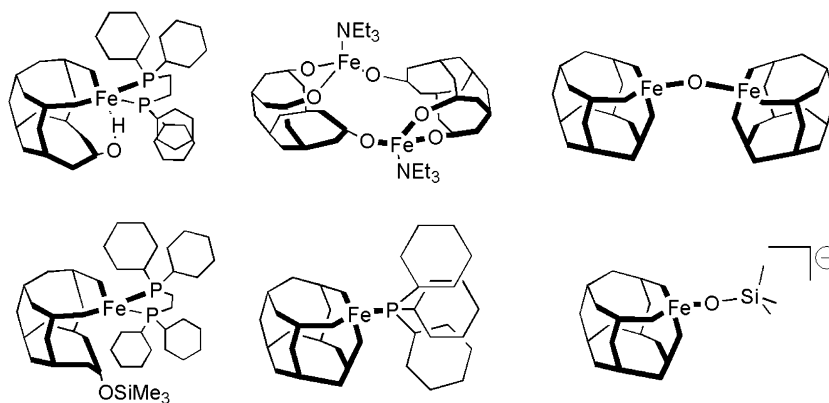


Chart 6. Fe-based silsesquioxanes.

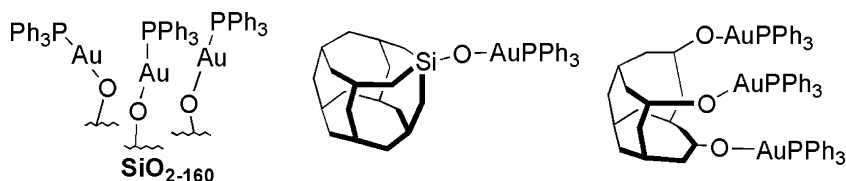


Chart 7. Silica-grafted Au(I) triphenylphosphine moieties and relevant silsesquioxane models.

lematic side reaction [136]. The alkyldiene bismonosilsesquioxane Mo(VI) complex  $[(C_5H_9)_7O_{12}Si_8O]_2Mo(=C-Et)(NtBuAr)(NhtBuAr)$  ( $Ar=C_6H_3Me_2$ ) has been synthesized and compares well to the analogous penta-coordinated silica-supported alkyne metathesis catalyst [136].

### 3.5. Group 7

#### 3.5.1. Olefin metathesis Re-carbene catalysts

The single-site product of the reaction of the perhydrocarbonyl Re(VII) complex  $[Re(-CH_2-tBu)_2(=CH-tBu)(=C-tBu)]$  with silica  $SiO_{2-700}$ ,  $[(=SiO)Re(=CH-tBu)(=C-tBu)]$ , a very active metathesis catalyst [137], is closely modelled by the reaction with the monosilanol silsesquioxane **1a** [138] and by the reaction with triphenylsilanol [137]. Similar to the surface data, the *syn* and *anti* isomers can be identified for the molecular models, the former giving rise to an H-agostic interaction [139]. The *syn* isomer appears as the sole surface species obtained in the grafting. Thermal or photochemical treatment is necessary to observe the *anti* rotamer on the surface in a 2:1 *syn:anti* ratio [138]. Conversely, the solution models yield directly a 10:1 mixture of the two rotamers by room temperature reaction in solution (Scheme 11). Such a difference points at the possibility to isolate on the surface a kinetic product before evolution to the thermodynamic most stable system occurs, which is usually observed in solution chemistry (and hence modelled with silsesquioxane). Such heterogeneous vs. homogeneous difference was already observed during the grafting of Mn(II)(TMEDA)bisneopentyl on silica and solution reaction of the same Mn(II) precursor with the silsesquioxane model **1** (yielding respectively a monografted monosiloxy tetrahedral Mn(II) and a bis-siloxy octahedral Mn(II), Scheme 11) [140].

### 3.6. Group 8

#### 3.6.1. Fe-based oxidation catalysts

Silica-supported iron materials catalyse oxidation reactions [141]. Fe(II) and Fe(III) silsesquioxanes are reported (Chart 6) [142,143], offering possible structural similarities with iron-zeolites in the ancillary ligand-free systems. Some of the Fe-POSS were tested in catalytic oxidation of benzene with  $N_2O$  with little success [143]. Successful examples of tethered Os(IV) complexes for dihydroxylation of alkenes are reported [144].

### 3.7. Group 9

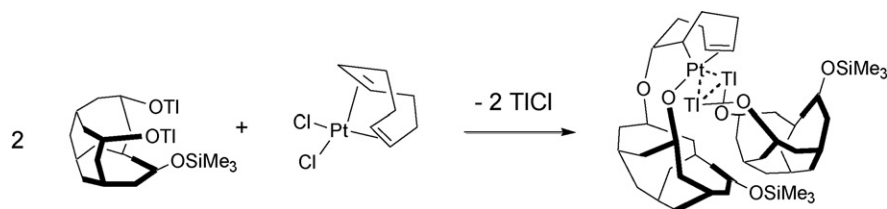
#### 3.7.1. Rhodium-based catalysts for hydroformylation

A surface-grafted phenylphosphane tether to the hydroformylation catalytic dinuclear Rh(II) precursor  $[Rh_2(m-P-C)_2(m-O_2CR)_2]$  (*m*-P-C-bridging ortho-metalated arylphosphine ligand) was modelled with a silsesquioxane analogue and displayed similar leaching issues [145].

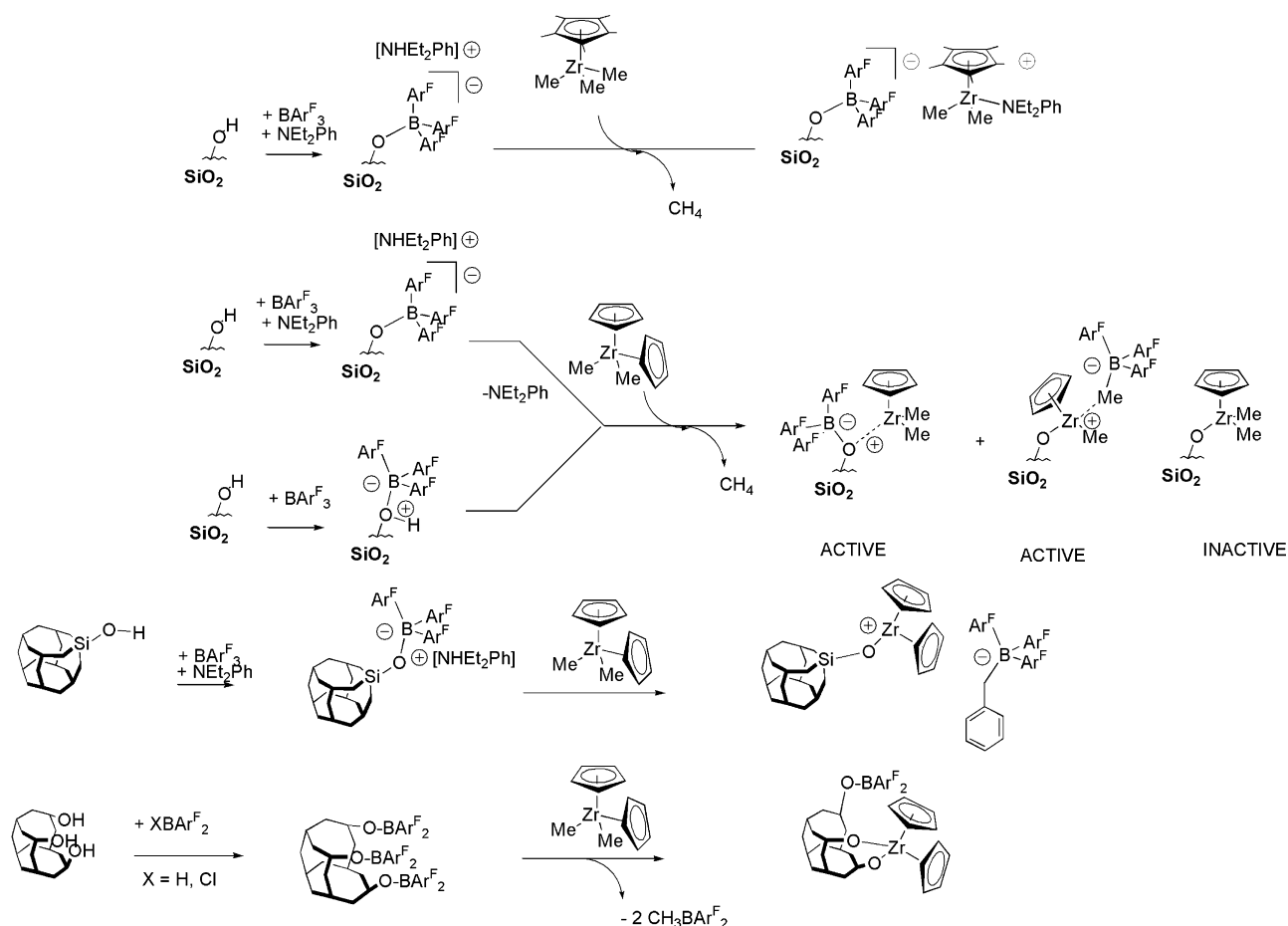
### 3.8. Group 10

#### 3.8.1. Platinum catalysts for hydrogenation

Platinum grafted on inorganic oxides is ubiquitous in heterogeneous catalysis, including hydrogenation of unsaturated organic substrates. An unusual silsesquioxane displaying an SiO–C linkage between the Feher cage **2b** and the partially hydrogenated cyclooctaenyl  $C_8$  organic linker of the organometallic Pt(COD)Cl<sub>2</sub> precursor has been reported [146], and proposed as a distant molecular model for putative non-innocent surface participation in Pt-catalyzed hydrogenation reactions (reaction (5)).



(5)



**Scheme 12.** Floating cationic Zr(IV) surface species obtained from  $\text{BAr}^{\text{F}}_3$  with silica followed by reaction with either  $\text{Cp}^*\text{ZrMe}_3$  or  $\text{Cp}_2\text{ZrMe}_2$ , and possible silsesquioxane models.

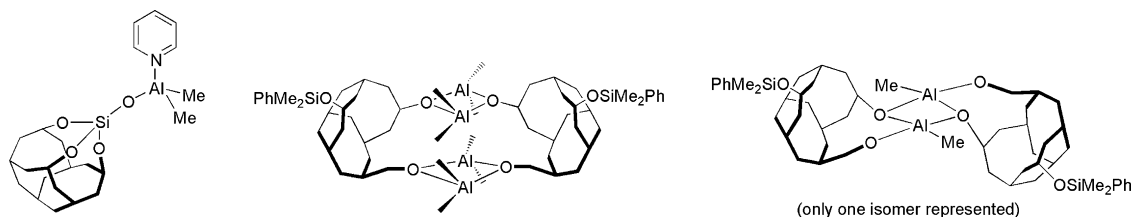


**Chart 8.** Silsesquioxane-based methylaluminosiloxane used as a co-catalyst in polymerization reactions.

### 3.9. Group 11

#### 3.9.1. Gold on silica catalysts

The catalytic relevance of gold nanoparticles or other highly dispersed forms of the noble metal supported on inorganic oxides is at the forefront of research [147–150]. This includes the microscopic understanding of the gold–substrate interaction in a number of Au/oxide systems (single atoms, two-dimensional islands, three-dimensional nanoparticles, etc.) [151]. A silsesquioxane model for the interaction of gold(I) precursor  $\text{Au}(\text{O}_2\text{CNEt}_2)(\text{PPh}_3)$  with silica surface previously dehydroxylated at  $160^\circ\text{C}$  has been reported, showing that **1a** can coordinate three gold molecules without inducing XPS detectable  $\text{Au}\cdots\text{Au}$  interactions (Chart 7) [152].

### 3.10. Group 12

#### 3.10.1. Zinc catalysts

A silica-supported zinc heterogeneous catalyst active in the copolymerization of cyclohexene oxide with  $\text{CO}_2$  was obtained by

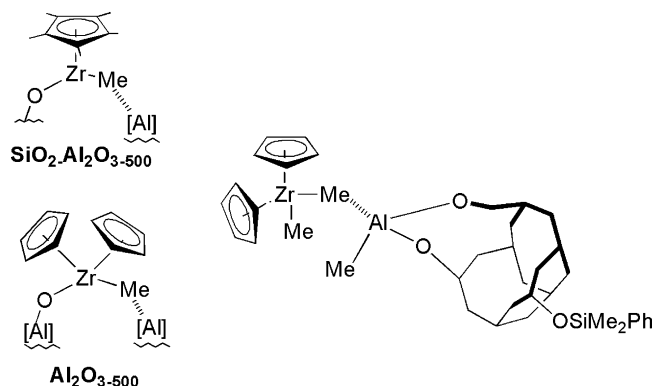


**Chart 9.** Analogy between the Lewis acid–base interaction observed for methyl zirconocene grafted on alumina and silica alumina and neighbouring surface acidic sites and  $\text{Cp}_2\text{ZrMe}_2$  interacting with aluminosilsesquioxane.



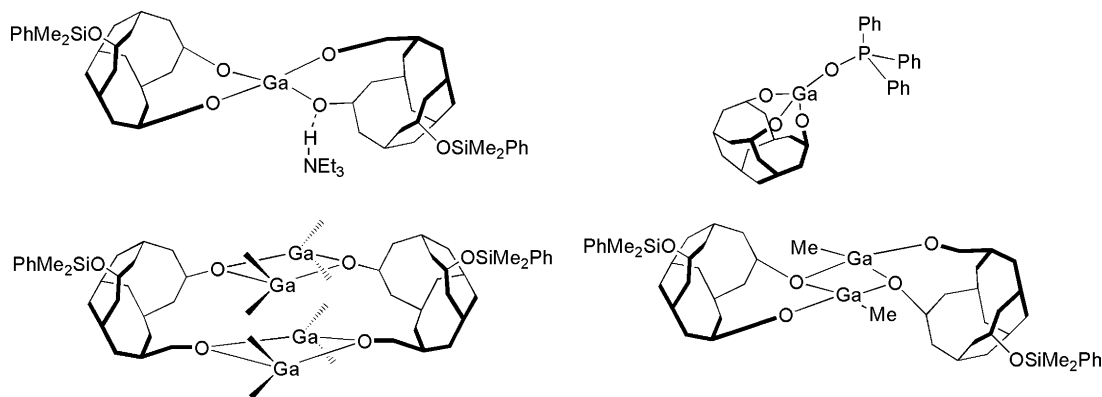


Chart 10. Examples of gallium silsesquioxanes.

reaction of  $\text{ZnEt}_2$  with mesoporous silica ( $\text{SiO}_{2-250}$ ); ICP-MS data suggest the formation of a bipodally grafted species [153]. Reaction of the dimethyl analogue  $\text{ZnMe}_2$  with silsesquioxane **2b** ( $\text{R} = \text{C}_5\text{H}_9$ ,  $\text{R}' = \text{SiMePh}_2$ ) gave the model  $[(\text{C}_5\text{H}_9)_7\text{Si}_7\text{O}_9(\text{MePh}_2)_2\text{O}_2\text{Zn}_2\text{Me}_2]_2$  which is also active in the copolymerization of cyclohexene and  $\text{CO}_2$  and resembles the molecular zinc bis phenoxide system [153].

### 3.11. Group 13

#### 3.11.1. Models of silica-grafted organoboranes for floating Zr polymerization catalysts

A successful route to heterogeneous floating Zr(IV) cationic metallocene for olefin polymerization catalysts has consisted in the use of organoborane modified silicas [86], which are obtained by pre-treatment of the silica with  $\text{BAR}^{\text{F}_3}$ , possibly in the presence of  $\text{Et}_2\text{NH}$ . In the case of  $\text{Cp}^*\text{ZrMe}_3$  it has lead to  $[(\equiv\text{SiO})\text{BAR}^{\text{F}_3}]^-[\text{Cp}^*\text{ZrMe}_2\text{NEt}_2\text{Ph}]^+$ , a moderately active ethylene polymerization catalyst [86] with an estimated activity of  $67 \text{ kg PE molZr}^{-1} \text{ atm}^{-1} \text{ bar}^{-1}$ . The same synthetic route with  $\text{Cp}_2\text{ZrMe}_2$  lead to the floating cationic species  $[(\equiv\text{SiO})\text{BAR}^{\text{F}_3}]^-[\text{Cp}_2\text{ZrMe}]^+$ . Such primary species undergoes surface ligand exchange to  $[(\equiv\text{SiO})\text{ZrCp}_2]^+[\text{MeBAR}^{\text{F}_3}]^-$ , thus ultimately weakening the catalytic activity of the resulting material [80]. The synthetic route to floating cationic Zr(IV) with organoborane-modified silica has been successfully modelled by silsesquioxane chemistry. The monopodal borato silsesquioxane complex  $[(\text{C}_5\text{H}_9)_7\text{Si}_7\text{O}_{12}\text{SiO}(\text{BAR}^{\text{F}_3})][\text{NH}(\text{Et})_2\text{Ph}]$  is obtained from the reaction of  $\text{BAR}^{\text{F}_3}$  with silsesquioxane **1a** in the presence of the amine [154] and it models the first step of the borane-modified silicas. The borato silsesquioxane reacts with  $\text{Cp}_2\text{Zr}(\text{CH}_2\text{Ph})_2$  to yield the active catalyst  $[(\text{C}_5\text{H}_9)_7\text{Si}_7\text{O}_{12}\text{SiOZrCp}_2][(\text{CH}_2\text{Ph})\text{BAR}^{\text{F}_3}]$  [154]. The borane-pretreated silica can also be modelled by triborane silsesquioxane  $[(\text{C}_5\text{H}_9)_7\text{Si}_7\text{O}_9(\text{O}(\text{BAR}^{\text{F}_2})_3)]$ , which reacts with  $\text{Cp}_2\text{ZrMe}_2$  to yield thermally unstable bimetallic complex  $[(\text{C}_5\text{H}_9)_7\text{Si}_7\text{O}_9(\text{O}(\text{BAR}^{\text{F}_2})_2)(\text{O}_2\text{ZrCp}_2)]$  (Scheme 12) [155].

Boron-containing silsesquioxanes have also been developed with their analogous Al and Ga-derivatives as models for group 13 element-doped zeolites [45] (Section 3.11.3).

#### 3.11.2. Al-based catalysts for polymerization

An ill-defined aluminum-based heterogeneous catalyst for *rac*-lactide ring opening polymerization in the melt was obtained by reaction of aluminum(III) isopropoxide with blandly dehydroxylated silica ( $\text{SiO}_{2-130}$ ) [156]. The alkyl-free aluminum dimer  $[(\text{Me}_2\text{CH})_7\text{O}_9\text{Si}_7\text{O}_3\text{Al}]_2$ , used as distant molecular model of the silica-supported system, catalyzes the same reaction, albeit with different activities (*viz.* yields = 5% vs. 10% yield after 48 h,  $M_N = 24,500$  vs. 3000; and  $M_W = 81,400$  vs. 4050, for the homo-

neous and heterogeneous systems, respectively) [156]. The absence of alkyl moieties in the silsesquioxane model further breaks down the analogy with the heterogeneous catalysts, for which a carbon content of 4% was measured, albeit no molecular proposal for the heterogeneous catalysts was put forward. *Rac*-lactide polymerization tests have been performed for the Ti-isopropoxide heterogeneous catalysts and its silsesquioxane models discussed in Section 3.2.1, with the homogeneous systems being more active [156].

Methyl aluminosilsesquioxane, potential models for MAO-modified silicas, were obtained from the reaction of  $\text{AlMe}_3$  with either the monosilanol **1a** in the presence of pyridine or the monosilylated disilanol **2b** ( $\text{R}' = \text{SiMe}_2\text{Ph}$ ). The final POSS:Al content depended, *inter alia*, on the stoichiometry of the reaction (Chart 8) [157].

The methylaluminosiloxanes have been tested as potential co-catalysts with, *inter alia*,  $\text{Cp}_2\text{ZrMe}_2$ , but were not Lewis-acidic enough to abstract the methyl and hence did not produce a potentially active polymerization catalyst. The one exception is the Brønsted acid derivative which gave clean transfer of the POSS on the Zr coordination sphere, still catalytically inactive. Reaction of the methylaluminosiloxane with  $\text{Cp}_2\text{ZrMe}_2$  lead to isomerisation of the silsesquioxanes to their thermodynamic mixture. The isomerisation suggests an acid–base interaction similar to the acid–base interaction between the acid surface aluminum sites and  $[(\equiv\text{SiO})\text{ZrMeCp}_2]^+$  moiety grafted on silica-alumina (Chart 9) [79].

#### 3.11.3. Ga-modified silsesquioxanes as models for doped zeolites

Gallium-modified zeolites catalyze light alkane transformation reactions such as cracking, dehydrogenation, and aromatization [158–160]. More generally, zeolites and silicates doped by an element of the group 13 can act as heterogeneous acidic catalysts and supports [45]. The modelling with silsesquioxane derivatives (Chart 10 for some examples) showed the relevance of protonolysis and salt metathesis reactions in their solution chemistry [45,161]. No catalytic data are reported.

### 3.12. Group 14

#### 3.12.1. Tin catalysts for oxidation

Tin-containing silicates and tin-grafted silicas are heterogeneous oxidation catalysts [162–164]. Model silsesquioxanes have highlighted a rich chemistry of tin silsesquioxanes with clusters of varying nuclearities [165] and Sn migration mechanisms [166]. No catalytic activity in oxidation reactions could be observed. Dialkyl tin(IV) disiloxy silsesquioxane, commercially sold as polyurethane cure catalysts, have been tested as homogeneous catalyst for urethane polymerization [167].

## 4. Conclusions

Silsesquioxane, if they had an inkling of personality, could claim some credit in the ongoing shrinking [1,168–171] of the heterogeneous–homogeneous gap in catalysis. As this review has shown, organometallic and inorganic derivatives of silsesquioxanes, familiarly called POSS, have been applied to a wide series of metals to better elucidate a range of heterogeneous catalytic reactions. These include, for example, titanium POSS-derivatives to gain insight in epoxidations with TS-1 [59–63], Zr-POSS applied to heterogeneous catalysts for hydrocarbon transformations [84] and esterification [108]; Cr- [123], V- [23,121], zirconium- [84] and boron- [155] containing POSS for olefins polymerization by silica-supported catalysts; Re- [138], W- [134], and Mo- [127] derivatives for olefin metathesis; Fe-POSS for oxidation; Al [39], Ga [45], or unsubstituted silsesquioxanes [32] for modelling various catalytic zeolites and other oxidic supports, etc.

We can summarize the contributions that silsesquioxane have offered to heterogeneous catalysis as threefold: (1) help in spectroscopic assignments of surface-bound organometallic and metal–inorganic fragments, (2) better understanding of elementary step and reaction mechanism(s) occurring at the surface, and (3) molecularly precise structure–activity insight for heterogeneous catalysts.

Regarding the first and historic application of POSS in the field, that is the contribution to spectroscopic assignments of surface-bound fragments, the contribution has been major and is slowly fading out except for multi-site heterogeneous systems where POSS still play a significant role.

Indeed, since their initial application in the field by Feher and his co-workers [32,83,123] to most recent examples almost 20 years later [63,119,134,153], silsesquioxanes have consistently proven to be valuable models for assigning structural and spectroscopic signatures of their silica-supported heterogeneous counterparts. For example, it has been possible to corroborate the solid-state  $^{13}\text{C}$  NMR signatures of metal alkylidene derivatives (not easily observable in the solid state) by direct comparison with the straightforwardly detectable carbenic signature in the liquid state NMR spectrum of the appropriate POSS molecule [130]. Limits to the usefulness of this contribution reside in the constant progress in solid-state techniques. In NMR spectroscopy for example, current state of the art MAS solid-state NMR multinuclear correlation techniques allows molecular-level precision such as, for example, measuring  $J_{\text{C-H}}$  coupling in agostically bonded methyllidene of Re(VII) neopentylidene metathesis heterogeneous catalyst [138] or counting the number of protons borne by one nitrogen atom on a surface complex after ammonia [172] or dinitrogen activation [173], thus eroding the competitive edge of homogeneous liquid state spectroscopy over the solid-state one.

In the case of multiple surface species, even with continuously more molecularly precise and performing solid-state analyses, the assignments of each single surface species to its own signals remains difficult. In this multi-site context, the silsesquioxanes still play a key role as standards with which to compare the spectroscopic features of the surface bound fragments. The approach relies, *inter alia*, on the availability of the various molecular mono-, di- or trisilanols of the silsesquioxane family which give the possibility to separately synthesize models of different surface species (mono-, di-, and tripodal surface species) possibly coexisting in the solid catalysts, and thus help to separately assign each respective spectroscopic signature [135].

Regarding the second contribution that POSS have given to heterogeneous catalysis, that is to better understand the elementary steps occurring on surface-bound organometallic and metal–inorganic fragments, examples span from the  $\alpha$ -H elimination of neopentane from Ta(V) neopentyl complexes [130,131], to

ligand exchange from siloxy borato to siloxy floating zirconocene complexes [154]. In all cases, the results have highlighted the validity of classical organometallic elementary steps in the comprehension of surface chemistry. Such contributions have also permitted a clearer relationship in molecular terms between surface reactivity and catalytic activity (or lack thereof) of the species, as discussed below.

Thirdly, and probably most interesting for core heterogeneous catalysis, it is possible to evaluate the catalytic activity of a single POSS derivative and compare it with the overall activity of the heterogeneous catalysts under study. The very fact that a POSS derivative is capable of reproducing a heterogeneous catalytic act while other molecular models, such as triphenylsilanol, might not is already insightful. For example, the successful modelling of the MAO-activated silica-supported vanadyl catalyst by trisiloxyl POSS – which the simpler  $(\text{Ph}_3\text{SiO})_3\text{V}=\text{O}$  cannot achieve – shows the capacity of POSS to mimic the catalytically necessary inter-atomic interactions found in the silica-supported catalyst (in this case V–Al) [112]. The structure–activity insight offered by POSS becomes particularly relevant for a complex multi-site heterogeneous catalyst, where most surface species are modelled separately one POSS analogue at the time, and an intrinsic catalytic activity can be assigned to each one of the surface species separately.

These three aspects (spectroscopic assignment, discrimination between different surface species and structure–activity correlation) with the final goal of optimizing the heterogeneous catalyst under study can indeed be treated in a single study. A valuable example is the elegant DR-UV study on epoxidation with a series of Ti-containing silicas, where the correlation between the catalytic activity and the Ti loading, type of silica, or silanization degree of various heterogeneous catalysts have been established and understood in molecular-terms thanks to comparison with several appropriate Ti-POSS [63]. Beside these positive contributions that POSS have offered to heterogeneous catalysis, the review has also shown some cases of silsesquioxanes inadequacy as molecular analogues to silica-bound fragments. The main limitation to the insight that silsesquioxane can offer to heterogeneous catalysis is when the analogy breaks down which sounds almost like a truism.

The analogy mostly breaks down when silsesquioxane can access a chemistry that heterogeneous catalysts cannot: for example, reaction with the solvent, dimerization [140] or other dinuclear deactivation routes inaccessible to sturdily monomeric immobilized silica-grafted species [127]. By the same token, observing the limits of silsesquioxane might be considered a way for assessing some of the advantages of heterogeneous catalysis (site isolation, lack of solvent deactivation, etc.).

In many instances, picket-fenced molecular models have proven more efficient than silsesquioxanes: for example, when POSS failed to stabilize highly electron deficient  $8e^-$  Zr(IV) species, claw-type trisamido molecules lead to isolable solution  $8e^-$  molecular species [104], showing that appropriate design of the molecular model can provide surprising and efficient heterogeneous–homogeneous analogies.

In conclusion, under the condition that the solution-only routes of decomposition are not available to POSS analogues (and thus no complications arise for the silica–silsesquioxane analogy to hold), the most insightful lesson from comparing model silsesquioxanes with the corresponding heterogeneous catalytic systems is, for us, that the activities are substantially the same. In a nut shell, for simple uncomplicated cases, the gap between heterogeneous catalysts and their model homogeneous analogues such as silsesquioxanes is not only reduced, it is non-existent. It does indeed make sense that when it boils down to making and breaking the same bonds under the same conditions, catalysis becomes one, with no distinction between heterogeneous and homogeneous. But rarely (if ever) does it boil down to that, summing up the value and limit

of silsesquioxanes' accuracy as molecular models for silica-grafted heterogeneous catalysts.

## References

- [1] C. Copéret, M. Chabanas, R.P. Saint-Arroman, J.-M. Basset, *Angew. Chem., Int. Ed.* 42 (2003) 156.
- [2] J.-P. Candy, C. Copéret, J.-M. Basset, *Top. Organomet. Chem.* 16 (2005) 151.
- [3] R. Murugavel, A. Voigt, M.G. Walawalkar, H.W. Roesky, *Chem. Rev.* 96 (1996) 2205.
- [4] B. Marciniak, H. Maciejewski, *Coord. Chem. Rev.* 223 (2001) 301.
- [5] C. Floriani, R. Floriani-Moro, *Adv. Organomet. Chem.* 47 (2001) 167.
- [6] C. Floriani, *Chem. Eur. J.* 5 (1999) 19.
- [7] C. Limberg, *Eur. J. Inorg. Chem.* (2007) 3303.
- [8] O.A. Kholdeeva, R.I. Maksimovskaya, *J. Mol. Catal. A: Chem.* 262 (2007) 7.
- [9] L.H. Gade, *Acc. Chem. Res.* 35 (2002) 575.
- [10] J.A. Tossell, *J. Phys. Chem. C* 111 (2007) 3584.
- [11] M. Sierka, J. Sauer, *Faraday Discuss.* 106 (1997) 41.
- [12] M.J. Janik, J. Macht, E. Iglesia, M. Neurock, *J. Phys. Chem. C* 113 (2009) 1872.
- [13] Y. Zhang, Z. Ye, *Chem. Commun.* (2008) 1178.
- [14] S.A. Raynor, J.M. Thomas, R. Raja, B.F.G. Johnson, R.G. Bell, M.D. Mantle, *Chem. Commun.* (2000) 1925.
- [15] J.R. Severn, R. Duchateau, R.A. Van Santen, D.D. Ellis, A.L. Spek, G.P.A. Yap, *Dalton Trans.* (2003) 2293.
- [16] H.C.L. Abbenhuis, *Chem. Eur. J.* 6 (2000) 25.
- [17] J.R. Severn, J.C. Chadwick, R. Duchateau, N. Friederichs, *Chem. Rev.* 105 (2005) 4073.
- [18] R. Duchateau, *Chem. Rev.* 102 (2002) 3525.
- [19] C. Copéret, J.M. Basset, *Adv. Synth. Catal.* 349 (2007) 78.
- [20] E.A. Quadrelli, in: J.M. Basset, R. Psaro, D. Roberto, R. Ugo (Eds.), *Modern Surface Organometallic Chemistry*, Wiley-VCH, 2009, p. 557.
- [21] P.P. Pescarmona, T. Maschmeyer, *Aust. J. Chem.* 54 (2001) 583.
- [22] V. Chandrasekhar, R. Boomishankar, S. Nagendran, *Chem. Rev.* 104 (2004) 5847.
- [23] F.J. Feher, T.A. Budzichowski, *Polyhedron* 14 (1995) 3239.
- [24] R.W.J. M. Hanssen, R.A. van Santen, H.C.L. Abbenhuis, *Eur. J. Inorg. Chem.* (2004) 675.
- [25] V. Lorenz, F.T. Edelmann, *Adv. Organomet. Chem.* 53 (2005) 101.
- [26] P.D. Lickiss, F. Rataboul, *Adv. Organomet. Chem.* 57 (2008) 1.
- [27] J.E. Mark, *Acc. Chem. Res.* 39 (2006) 881.
- [28] F.J. Feher, R. Terroba, R.-Z. Jin, K.D. Wyndham, S. Lucke, R. Brutchey, F. Nguyen, *Polym. Mater. Sci. Eng.* 82 (2000) 301.
- [29] A.P. Legrand (Ed.), *The Surface Properties of Silicas*, Wiley, 1998.
- [30] E.F. Vansant, P. Van Der Voort, K.C. Vrancken (Eds.), *Stud. Surf. Sci. Catal.* 93 (1995).
- [31] E. Groppo, C. Lamberti, S. Bordiga, G. Spoto, A. Zecchina, *Chem. Rev.* 105 (2005) 115.
- [32] F.J. Feher, D.A. Newman, J.F. Walzer, *J. Am. Chem. Soc.* 111 (1989) 1741.
- [33] F.J. Feher, D.A. Newman, *J. Am. Chem. Soc.* 112 (1990) 1931.
- [34] T.W. Dijkstra, R. Duchateau, R.A. van Santen, A. Meetsma, G.P.A. Yap, *J. Am. Chem. Soc.* 124 (2002) 9856.
- [35] R. Duchateau, H.C.L. Abbenhuis, R.A. Van Santen, S.K.H. Thiele, M.F.H. Van Tol, *Organometallics* 17 (1998) 5222.
- [36] L.T. Zhuravlev, *Langmuir* 3 (1987) 316.
- [37] R. Duchateau, T.W. Dijkstra, R.A. van Santen, G.P.A. Yap, *Chem. Eur. J.* 10 (2004) 3979.
- [38] F.J. Feher, T.A. Budzichowski, K. Rahimian, J.W. Ziller, *J. Am. Chem. Soc.* 114 (1992) 3859.
- [39] F.J. Feher, T.A. Budzichowski, K.J. Weller, *J. Am. Chem. Soc.* 111 (1989) 7288.
- [40] F.J. Feher, K.J. Weller, *Organometallics* 9 (1990) 2638.
- [41] R. Duchateau, R.J. Harmsen, H.C.L. Abbenhuis, R.A. Van Santen, A. Meetsma, S.K.H. Thiele, M. Kranenburg, *Chem. Eur. J.* 5 (1999) 3130.
- [42] F.T. Edelmann, Y.K. Gun'ko, S. Giessmann, F. Olbrich, K. Jacob, *Inorg. Chem.* 38 (1999) 210.
- [43] R.W. Joyner, A.D. Smith, M. Stockenhuber, M.W.E. van den Berg, *Phys. Chem. Chem. Phys.* 6 (2004) 5435.
- [44] S. Krijnen, R.J. Harmsen, H.C.L. Abbenhuis, J.H.C. Van Hooff, R.A. Van Santen, *Chem. Commun.* (1999) 501.
- [45] G. Gerritsen, R. Duchateau, R.A. van Santen, G.P.A. Yap, *Organometallics* 22 (2003) 100.
- [46] R.M. Gauvin, L. Delevoye, R.A. Hassan, J. Keldenich, A. Mortreux, *Inorg. Chem.* 46 (2007) 1062.
- [47] R.M. Gauvin, T. Chenal, R.A. Hassan, A. Addad, A. Mortreux, *J. Mol. Catal. A: Chem.* 257 (2006) 31.
- [48] R. Anwender, O. Runte, J. Eppinger, G. Gerstberger, E. Herdtweck, M. Spiegler, *J. Chem. Soc., Dalton Trans.* (1998) 847.
- [49] J. Annand, H.C. Aspinall, *Dalton Trans.* (2000) 1867.
- [50] V. Lorenz, S. Giessmann, Y.K. Gun'ko, A.K. Fischer, J.W. Gilje, F.T. Edelmann (Eds.), *Angew. Chem., Int. Ed.* 43 (2004) 4603.
- [51] G. Gerstberger, C. Palm, R. Anwender, *Chem. Eur. J.* 5 (1999) 997.
- [52] V. Lorenz, A. Fischer, F.T. Edelmann, *J. Organomet. Chem.* 647 (2002) 245.
- [53] T. Maschmeyer, F. Rey, G. Sankar, J.M. Thomas, *Nature* 378 (1995) 159.
- [54] G. Bellussi, M.S. Rigutto, *Stud. Surf. Sci. Catal.* 85 (1994) 177.
- [55] D. Gleeson, G. Sankar, C.R.A. Catlow, J.M. Thomas, G. Spano, S. Bordiga, A. Zecchina, C. Lamberti, *Phys. Chem. Chem. Phys.* 2 (2000) 4812.
- [56] P.E. Sinclair, G. Sankar, C.R.A. Catlow, J.M. Thomas, T. Maschmeyer, *J. Phys. Chem. B* 101 (1997) 4232.
- [57] J.M. Thomas, G. Sankar, M.C. Klunduk, M.P. Attfield, T. Maschmeyer, B.F.G. Johnson, R.G. Bell, *J. Phys. Chem. B* 103 (1999) 8809.
- [58] L. Marchese, T. Maschmeyer, E. Gianotti, S. Coluccia, J.M. Thomas, *J. Phys. Chem. B* 101 (1997) 8836.
- [59] M. Crocker, R.H.M. Herold, A.G. Orpen, *Chem. Commun.* (1997) 2411.
- [60] T. Maschmeyer, M.C. Klunduk, C.M. Martin, D.S. Shephard, J.M. Thomas, B.F.G. Johnson, *Chem. Commun.* (1997) 1847.
- [61] M. Crocker, R.H.M. Herold, A.G. Orpen, M.T.A. Overgaag, *J. Chem. Soc., Dalton Trans.* (1999) 3791.
- [62] M.C. Klunduk, T. Maschmeyer, J.M. Thomas, B.F.G. Johnson, *Chem. Eur. J.* 5 (1999) 1481.
- [63] J.M. Fraile, J.I. Garcia, J.A. Mayoral, E. Vispe, *J. Catal.* 233 (2005) 90.
- [64] A.O. Boud, G.L. Rice, S.L. Scott, *J. Am. Chem. Soc.* 121 (1999) 7201.
- [65] R.D. Oldroyd, G. Sankar, J.M. Thomas, D. Oezkaya, *J. Phys. Chem. B* 102 (1998) 1849.
- [66] Y. Perez, D.P. Quintanilla, M. Fajardo, I. Sierra, I. del Hierro, *J. Mol. Catal. A: Chem.* 271 (2007) 227.
- [67] G.G. Hlatky, *Chem. Rev.* 100 (2000) 1347.
- [68] K. Soga, Y. Suzuki, T. Uozumi, E. Kaji, *J. Polym. Sci. A: Polym. Chem.* 35 (1997) 291.
- [69] R. Duchateau, U. Cremer, R.J. Harmsen, S.I. Mohamud, H.C.L. Abbenhuis, R.A. Van Santen, A. Meetsma, S.K.H. Thiele, M.F.H. Van Tol, M. Kranenburg, *Organometallics* 18 (1999) 5447.
- [70] K. Soga, D.H. Lee, *Makromol. Chem.* 193 (1992) 1687.
- [71] R. Guimaraes, F.C. Stedile, J.H.Z. dos Santos, *J. Mol. Catal. A: Chem.* 206 (2003) 353.
- [72] K. Kageyama, J.-I. Tamazawa, T. Aida, *Science* 285 (1999) 2113.
- [73] S. Collins, W.M. Kelly, D.A. Holden, *Macromolecules* 25 (1992) 1780.
- [74] I.E. Buys, T.W. Hambley, D.J. Houlton, T. Maschmeyer, A.F. Masters, A.K. Smith, *J. Mol. Catal.* 86 (1994) 309.
- [75] F.T. Edelmann, S. Giessmann, A. Fischer, *J. Organomet. Chem.* 620 (2001) 80.
- [76] W. Kaminsky, A. Laban, *J. Appl. Catal. A* 222 (2001) 47.
- [77] E.Y.-X. Chen, T.J. Marks, *Chem. Rev.* 100 (2000) 1391.
- [78] T.J. Marks, *Acc. Chem. Res.* 25 (1992) 57.
- [79] M. Jezequel, V. Dufaud, M.J. Ruiz-Garcia, F. Carrillo-Hermosilla, U. Neugebauer, G.P. Niccolai, F. Lefebvre, F. Bayard, J. Corker, S. Fiddy, J. Evans, J.-P. Broyer, J. Malinge, J.-M. Basset, *J. Am. Chem. Soc.* 123 (2001) 3520.
- [80] N. Millot, S. Soignier, C.C. Santini, A. Baudouin, J.-M. Basset, *J. Am. Chem. Soc.* 128 (2006) 9361.
- [81] P.G. Bellelli, A. Eberhardt, M.L. Ferreira, V.C. Vaya, J.H.Z. Dos Santos, D.E. Damiani, *Curr. Trends Polym. Sci.* 5 (2000) 79.
- [82] S.R. Loureiro, F. Silveira, G.P. Pires, M.D.C. Alves, F.C. Stedile, J.H.Z. Dos Santos, K.M. Bichinho, T. Teranishi, X-Ray Spectrom. 34 (2005) 101.
- [83] F.J. Feher, *J. Am. Chem. Soc.* 108 (1986) 3850.
- [84] R. Duchateau, H.C.L. Abbenhuis, R.A. van Santen, A. Meetsma, S.K.H. Thiele, M.F.H. van Tol, *Organometallics* 17 (1998) 5663.
- [85] C. Pellecchia, A. Grassi, A. Zambelli, *J. Mol. Catal.* 82 (1993) 57.
- [86] J. Tian, S. Wang, Y. Feng, J. Li, S. Collins, *J. Mol. Catal. A: Chem.* 144 (1999) 137.
- [87] J.R. Severn, R. Duchateau, R.A. van Santen, D.D. Ellis, A.L. Spek, *Organometallics* 21 (2002) 4.
- [88] N. Kashiwa, *J. Polym. Sci. A: Polym. Chem.* 42 (2003) 1.
- [89] S.H. Kim, G.A. Somorjai, *Surf. Interface Anal.* 31 (2001) 701.
- [90] F.J. Feher, J.F. Walzer, *Inorg. Chem.* 29 (1990) 1604.
- [91] D.G. Ward, *WO Patent Appl.* 9,613,531 (1996).
- [92] J.-C. Liu, *Chem. Commun.* (1996) 1109.
- [93] R. Duchateau, *Nanostruct. Catal.* (2003) 57.
- [94] F. Bini, C. Rosier, R.P. Saint-Arroman, E. Neumann, C. Dablemont, A. de Mallmann, F. Lefebvre, G.P. Niccolai, J.-M. Basset, M. Crocker, J.-K. Buijink, *Organometallics* 25 (2006) 3743.
- [95] F. Quignard, C. Lecuyer, C. Bougault, F. Lefebvre, A. Choplin, D. Olivier, J.M. Basset, *Inorg. Chem.* 31 (1992) 928.
- [96] V.A. Zakharov, V.K. Dudchenko, E. Paukstis, L.G. Karakchiev, Y.I. Ermakov, *J. Mol. Catal.* 2 (1977) 421.
- [97] F. Rataboul, A. Baudouin, C. Thieuleux, L. Veyre, C. Copéret, J. Thivolle-Cazat, J.-M. Basset, A. Lesage, L. Emsley, *J. Am. Chem. Soc.* 126 (2004) 12541.
- [98] C. Thieuleux, E.A. Quadrelli, J.-M. Basset, J. Doeblér, J. Sauer, *Chem. Commun.* (2004) 1729.
- [99] F. Quignard, A. Choplin, J.-M. Basset, *J. Chem. Soc., Dalton Trans.* (1994) 2411.
- [100] J. Schwartz, M.D. Ward, *J. Mol. Catal.* 8 (1980) 465.
- [101] C. Lecuyer, F. Quignard, A. Choplin, D. Olivier, J.M. Basset, *Angew. Chem.* 103 (1991) 1692.
- [102] J. Corker, F. Lefebvre, C. Lecuyer, V. Dufaud, F. Quignard, A. Choplin, J. Evans, J.-M. Basset, *Science* 271 (1996) 966.
- [103] V. Dufaud, J.-M. Basset (Eds.), *Angew. Chem., Int. Ed.* 37 (1998) 806.
- [104] L. Jia, E. Ding, A.L. Rheingold, B. Rhatigan, *Organometallics* 19 (2000) 963.
- [105] G. Tosin, C.C. Santini, A. Baudouin, A. De Mallman, S. Fiddy, C. Dablemont, J.-M. Basset, *Organometallics* 26 (2007) 4118.
- [106] G. Tosin, C.C. Santini, M. Taoufik, A. De Mallmann, J.-M. Basset, *Organometallics* 25 (2006) 3324.
- [107] N. Ferret, V. Dufaud, V. Salinier, J.-M. Basset, *Fr. Patent Appl.* 2,747,675 (1997).
- [108] V. Salinier, G.P. Niccolai, V. Dufaud, J.-M. Basset, *Adv. Synth. Catal.* 351 (2009) 2168–2177.
- [109] N. Das, H. Eckert, H. Hu, I.E. Wachs, J.F. Walzer, F.J. Feher, *J. Phys. Chem.* 97 (1993) 8240.

- [110] K. Wada, M. Nakashita, A. Yamamoto, T. Mitsudo, *Chem. Commun.* (1998) 133.
- [111] F.J. Feher, J.F. Walzer, *Inorg. Chem.* 30 (1991) 1689.
- [112] F.J. Feher, J.F. Walzer, R.L. Blanski, *J. Am. Chem. Soc.* 113 (1991) 3618.
- [113] D.E. Keller, T. Visser, F. Soulimani, D.C. Koningsberger, B.M. Weckhuysen, *Vib. Spectrosc.* 43 (2007) 140.
- [114] D.E. Keller, S.M.K. Airaksinen, A.O. Krause, B.M. Weckhuysen, D.C. Koningsberger, *J. Am. Chem. Soc.* 129 (2007) 3189.
- [115] G.L. Rice, S.L. Scott, *J. Mol. Catal. A: Chem.* 125 (1997) 73.
- [116] G.L. Rice, S.L. Scott, *Langmuir* 13 (1997) 1545.
- [117] K. Inumaru, T. Okuhara, M. Misono, N. Matsubayashi, H. Shimada, A. Nishijima, *J. Chem. Soc., Faraday Trans.* 88 (1992) 625.
- [118] J. Keranen, C. Guimon, E. Iiskola, A. Auroux, L. Niinisto, *J. Phys. Chem. B* 107 (2003) 10773.
- [119] C. Ohde, M. Brandt, C. Limberg, J. Doeblner, B. Ziemer, J. Sauer, *Dalton Trans.* (2008) 326.
- [120] K. Wada, M. Nakashita, A. Yamamoto, H. Wada, T.-A. Mitsudo, *Chem. Lett.* (1997) 1209.
- [121] F.J. Feher, R.L. Blanski, *J. Am. Chem. Soc.* 114 (1992) 5886.
- [122] G. Sankar, J.M. Thomas, C.R.A. Catlow, C.M. Barker, D. Gleeson, N. Kaltsoyannis, *J. Phys. Chem. B* 105 (2001) 9028.
- [123] F.J. Feher, R.L. Blanski, *J. Chem. Soc., Chem. Commun.* (1990) 1614.
- [124] F.J. Feher, K. Rahimian, T.A. Budzichowski, J.W. Ziller, *Organometallics* 14 (1995) 3920.
- [125] I.J. Shannon, T. Maschmeyer, R.D. Oldroyd, G. Sankar, J. Meurig Thomas, H. Pernot, J.-P. Balikdjian, M. Che, *J. Chem. Soc., Faraday Trans.* 94 (1998) 1495.
- [126] W.A. Herrmann, S. Bogdanovic, R. Poli, T. Priermeier, *J. Am. Chem. Soc.* 116 (1994) 4989.
- [127] F. Blanc, M. Chabanas, C. Copéret, B. Fenet, E. Herdweck, *J. Organomet. Chem.* 690 (2005) 5014.
- [128] W.A. Herrmann, A.W. Stumpp, T. Priermeier, S. Bogdanovic, V. Dufaud, J.-M. Basset, *Angew. Chem., Int. Ed. Engl.* 35 (1997) 2803.
- [129] V. Dufaud, G.P. Niccolai, J. Thivolle-Cazat, J.-M. Basset, *J. Am. Chem. Soc.* 117 (1995) 4288.
- [130] M. Chabanas, E.A. Quadrelli, B. Fenet, C. Copéret, J. Thivolle-Cazat, J.-M. Basset, A. Lesage, L. Emsley, *Angew. Chem., Int. Ed.* 40 (2001) 4493.
- [131] E.L. Le Roux, M. Chabanas, A. Baudouin, A. de Mallmann, C. Copéret, E.A. Quadrelli, J. Thivolle-Cazat, J.-M. Basset, W. Lukens, A. Lesage, L. Emsley, G.J. Sunley, *J. Am. Chem. Soc.* 126 (2004) 13391.
- [132] F. Blanc, C. Copéret, J. Thivolle-Cazat, J.-M. Basset, A. Lesage, L. Emsley, A. Sinha, R.R. Schrock, *Angew. Chem., Int. Ed.* 45 (2006) 1216.
- [133] F.J. Feher, T.L. Tajima, *J. Am. Chem. Soc.* 116 (1994) 2145.
- [134] B. Rhers, A. Salameh, A. Baudouin, E.A. Quadrelli, M. Taoufik, C. Copéret, F. Lefebvre, J.-M. Basset, X. Solans-Monfort, O. Eisenstein, W.W. Lukens, L.P.H. Lopez, A. Sinha, R.R. Schrock, *Organometallics* 25 (2006) 3554.
- [135] B. Rhers, E.A. Quadrelli, A. Baudouin, M. Taoufik, C. Copéret, F. Lefebvre, J.-M. Basset, B. Fenet, A. Sinha, R.R. Schrock, *J. Organomet. Chem.* 691 (2006) 5448.
- [136] H. Weissman, K.N. Plunkett, J.S. Moore, *Angew. Chem., Int. Ed.* 45 (2006) 585.
- [137] M. Chabanas, A. Baudouin, C. Copéret, J.-M. Basset, *J. Am. Chem. Soc.* 123 (2001) 2062.
- [138] M. Chabanas, A. Baudouin, C. Copéret, J.-M. Basset, W. Lukens, A. Lesage, S. Hediger, L. Emsley, *J. Am. Chem. Soc.* 125 (2003) 492.
- [139] A. Lesage, L. Emsley, M. Chabanas, C. Copéret, J.-M. Basset, *Angew. Chem., Int. Ed.* 41 (2002) 4535.
- [140] V. Riollot, E.A. Quadrelli, C. Copéret, J.-M. Basset, R.A. Andersen, K. Kohler, R.-M. Bottcher, E. Herdtweck, *Chem. Eur. J.* 11 (2005) 7358.
- [141] G.I. Panov, A.K. Uriarte, M.A. Rodkin, V.I. Sobolev, *Catal. Today* 41 (1998) 365.
- [142] P.A. Shapley, W.S. Bigham, M.T. Hay, *Inorg. Chim. Acta* 345 (2003) 255.
- [143] F. Liu, K.D. John, B.L. Scott, R.T. Baker, K.C. Ott, W. Tumas, *Angew. Chem., Int. Ed.* 39 (2000) 3127.
- [144] P.P. Pescarmona, A.F. Masters, J.C. van der Waal, T. Maschmeyer, *J. Mol. Catal. A: Chem.* 220 (2004) 37.
- [145] M. Nowotny, T. Maschmeyer, B.F.G. Johnson, P. Lahuerta, J.M. Thomas, J.E. Davies, *Angew. Chem., Int. Ed.* 40 (2001) 955.
- [146] E.A. Quadrelli, J.E. Davies, B.F.G. Johnson, N. Feeder, *Chem. Commun.* (2000) 1031.
- [147] M. Haruta, *Stud. Surf. Sci. Catal.* 145 (2003) 31.
- [148] M. Haruta, *Cattech* 6 (2002) 102.
- [149] G.J. Hutchings, M. Brust, H. Schmidbaur, *Chem. Soc. Rev.* 37 (2008) 1759.
- [150] J.C. Fierro-Gonzalez, B.C. Gates, *Chem. Soc. Rev.* 37 (2008) 2127.
- [151] T. Risse, S. Shaikhutdinov, N. Nilius, M. Sterrer, H.-J. Freund, *Acc. Chem. Res.* 41 (2008) 949.
- [152] L. Abis, L. Armelao, D. Belli Dell'Amico, F. Calderazzo, F. Garbassi, A. Merigo, E.A. Quadrelli, *J. Chem. Soc., Dalton Trans.* (2001) 2704.
- [153] R. Duchateau, W.J. Van Meerendonk, S. Huijser, B.B.P. Staal, M.A. Van Schilt, G. Gerritsen, A. Meetsma, C.E. Koning, M.F. Kemmere, J.T.F. Keurentjes, *Organometallics* 26 (2007) 4204.
- [154] R. Duchateau, R.A. Van Santen, G.P.A. Yap, *Organometallics* 19 (2000) 809.
- [155] R.A. Metcalfe, D.I. Kreller, J. Tian, H. Kim, N.J. Taylor, J.F. Corrigan, S. Collins, *Organometallics* 21 (2002) 1719.
- [156] M.D. Jones, M.G. Davidson, C.G. Keir, A.J. Wooles, M.F. Mahon, D.C. Apperley, *Dalton Trans.* (2008) 3655.
- [157] M.D. Skowronska-Ptasinska, R. Duchateau, R.A. van Santen, G.P.A. Yap, *Organometallics* 20 (2001) 3519.
- [158] N. Rane, M. Kersbulck, R.A. van Santen, E.J.M. Hensen, *Micropor. Mesopor. Mater.* 110 (2008) 279.
- [159] E.A. Pidko, E.J.M. Hensen, R.A. Van, Santen, *J. Phys. Chem. C* 111 (2007) 13068.
- [160] D.B. Lukyanov, T. Vazhnova, *J. Appl. Catal. A* 316 (2006) 61.
- [161] F.J. Feher, T.A. Budzichowski, J.W. Ziller, *Inorg. Chem.* 36 (1997) 4082.
- [162] M. Boronat, P. Concepcion, A. Corma, M. Renz, *Catal. Today* 121 (2007) 39.
- [163] A. Corma, H. Garcia, *Chem. Rev.* 102 (2002) 3837.
- [164] E. Janiszewska, S. Kowalak, W. Supronowicz, F. Roessner, *Micropor. Mesopor. Mater.* 117 (2008) 423.
- [165] R. Duchateau, T.W. Dijkstra, J.R. Severn, R.A. van Santen, I.V. Korobkov, *Dalton Trans.* (2004) 2677.
- [166] C. Nedež, V. Dufaud, F. Lefebvre, J.-M. Basset, B. Fenet, *C. R. Chim.* 7 (2004) 785.
- [167] W. Wang, J.S. Wiggins, *J. Appl. Polym. Sci.* 110 (2008) 3683.
- [168] H.-J. Freund, *Catal. Today* 100 (2005) 3.
- [169] J. Matthes, T. Pery, S. Gruendemann, G. Buntkowsky, S. Sabo-Etienne, B. Chaudret, H.-H. Limbach, *J. Am. Chem. Soc.* 126 (2004) 8366.
- [170] A. Corma, *Catal. Rev. Sci. Eng.* 46 (2004) 369.
- [171] R.A. Van Santen, *Chem. Eng. Sci.* 50 (1995) 4027.
- [172] P. Avenier, A. Lesage, M. Taoufik, A. Baudouin, A. De Mallmann, S. Fiddy, M. Vautier, L. Veyre, J.-M. Basset, L. Emsley, E.A. Quadrelli, *J. Am. Chem. Soc.* 129 (2007) 176.
- [173] P. Avenier, M. Taoufik, A. Lesage, X. Solans-Monfort, A. Baudouin, A. de Mallmann, L. Veyre, J.M. Basset, O. Eisenstein, L. Emsley, E.A. Quadrelli, *Science* 317 (2007) 1056.